

## REVIEW ARTICLE

OPEN

## Green flexible electronics based on starch

Huacui Xiang<sup>1</sup>, Zhijian Li<sup>1</sup>, Hanbin Liu<sup>1</sup>✉, Tao Chen<sup>1</sup>✉, Hongwei Zhou<sup>3</sup> and Wei Huang<sup>1</sup>✉

Flexible electronics (FEs) with excellent flexibility or foldability may find widespread applications in the wearable devices, artificial intelligence (AI), Internet of Things (IoT), and other areas. However, the widely utilization may also bring the concerning for the fast accumulation of electronic waste. Green FEs with good degradability might supply a way to overcome this problem. Starch, as one of the most abundant natural polymers, has been exhibiting great potentials in the development of environmental-friendly FEs due to its inexpensiveness, good processability, and biodegradability. Lots of remarks were made this field but no summary was found. In this review, we discussed the preparation and applications of starch-based FEs, highlighting the role played by the starch in such FEs and the impacts on the properties. Finally, the challenge was discussed and the outlook for the further development was also presented.

*npj Flexible Electronics* (2022)6:15; <https://doi.org/10.1038/s41528-022-00147-x>

## INTRODUCTION

More than 100 years have passed since human walked from vacuum tubes to transistors. Nowadays, electronic devices are transforming from solid, durable, single-shape styles to wearable, versatile, high-performance, and multifunctional components, among which the flexible electronics (FEs) have already sprung up and gained extensive attentions<sup>1–4</sup>. The appealing applications of FEs may at least include personalized mobile devices, healthcare systems, human-machine interfaces, soft robots, electronic skin, artificial intelligence (AI), and Internet of Things (IoT)<sup>5–8</sup>. To fabricate FEs, the soft, stretchable, foldable substrates are highly desired. In general protocols, electro-conducting materials including metals, conducting polymers, or carbon-based materials are assembled on the flexible substrates, which involves polymer films such as polyethylene terephthalate (PET)<sup>9</sup>, polyimide (PI)<sup>10,11</sup>, hydrogels<sup>12</sup>, textiles<sup>13</sup>, and elastomers such as polydimethylsiloxane (PDMS)<sup>14,15</sup>. Nevertheless, these substrates are usually non-degradable, which may result in accumulation of electronic waste (e-waste). In estimation, the globe production of e-waste reached to 53.6 million tons by 2020, an average of 7.3 kg of one person. And this number might increase to 74.7 million tons by 2030<sup>16</sup>. In 2019, only 17.4% of the e-waste was recycled due to the tedious process and imperfect policy. Green FEs with good degradability may supply a way to fundamentally solve the problem.

In recent years, a variety of environment-friendly, bio-degradable, and low-cost electronic products have emerged<sup>17,18</sup>, which were made of materials from nature, including cellulose<sup>19–24</sup>, lignin<sup>25–29</sup>, proteins<sup>30–32</sup>, and starch<sup>33–35</sup>. These materials from nature have intrinsic advantages of abundant sources, low cost, good degradability, acceptable biocompatibility, fine accessibility for chemical modification comparing with synthesized polymers. They can be safely and bio-compatibly used as implantable devices for human healthcare and medical diagnose<sup>36</sup>. Furthermore, their utilization may be free of e-waste production to satisfy the requirements of the e-waste reduction.

Among the reported sustainable materials used in FEs, starch have advantages on the acceptable solubility in water, good property of film forming and relative low cost comparing with

cellulose, lignin and proteins. Therefore, a lot of efforts have been put into the developments of FEs based on starch<sup>37–41</sup>, in which the starch usually appeared as films or gels. The starch films were often used as soft and transparent substrates because of the intrinsic good film-forming property of starch. The conductive materials can be easily coated or printed on the starch film to fabricate FEs. On contrary, the starch hydrogel can be feasibly processed to various shapes with injection or 3D printing, which may further carbonize into conductive materials with stereoscopic structures. The water containing system of the hydrogel may also benefit for their biomedical application.

Though the starch films and gels have their own features, both were versatile in the exploration of FEs, such as flexible conductive electrodes, sensors, supercapacitors, transistors, and resistive switching memory devices (Fig. 1). However, to the best of our knowledge, no summary on this exciting area was found. Therefore, here in this review, the fundamentals and advantage of the starch used for FEs were firstly discussed. Subsequently, the starch-based devices were divided into two categories and successively summarized, i.e., FEs based on starch films vs FEs based on starch gels. The strategies of the preparation were introduced and the role of the starch played in these FEs was highlighted. The challenges and future prospects were finally addressed to end the review.

Starch is a natural-derived polysaccharide comprising of glucose monomers, which can be abundantly harvested from the roots, stems, and seeds of the rice, corns, wheat, cassavas, potatoes, and other crops. According to the molecular chain structure, the starch can be divided into amylose and amylopectin<sup>42–44</sup>. In the natural starch, amylose accounts for 20~26%, and the rest are amylopectin. The amylose has a linear monomer at chain with only  $\alpha$ -1,4 linkages thus possessing good extensibility in solution and can easily associate with some polar organic compounds by hydrogen bond. The amylopectin is the branch form with  $\alpha$ -1,4 linkages in the backbone and  $\alpha$ -1,6 linkages at the branched points, which usually has much higher molecular weight<sup>45</sup>. In addition, starch molecules contain lots of hydroxyl groups that are suitable for esterification<sup>46</sup>, etherification<sup>47</sup>, grafting<sup>48</sup>, cross-linking<sup>49</sup>, and

<sup>1</sup>Shaanxi Provincial Key Laboratory of Papermaking Technology and Specialty Paper Development, College of Bioresource Chemical and Materials Engineering, Shaanxi University of Science & Technology, Xi'an 710021, P.R. China. <sup>2</sup>Ningbo Institute of Materials Technology and Engineering, Chinese Academy of Sciences, Ningbo 315201, P.R. China. <sup>3</sup>School of Materials and Chemical Engineering, Xi'an Technological University, Xi'an 710021, P. R. China. <sup>4</sup>Frontiers Science Center for Flexible Electronics, Xi'an Institute of Flexible Electronics (IFE), Northwestern Polytechnical University, Xi'an 710072, China. ✉email: liuhanbin@sust.edu.cn; iamwhuang@nwpu.edu.cn

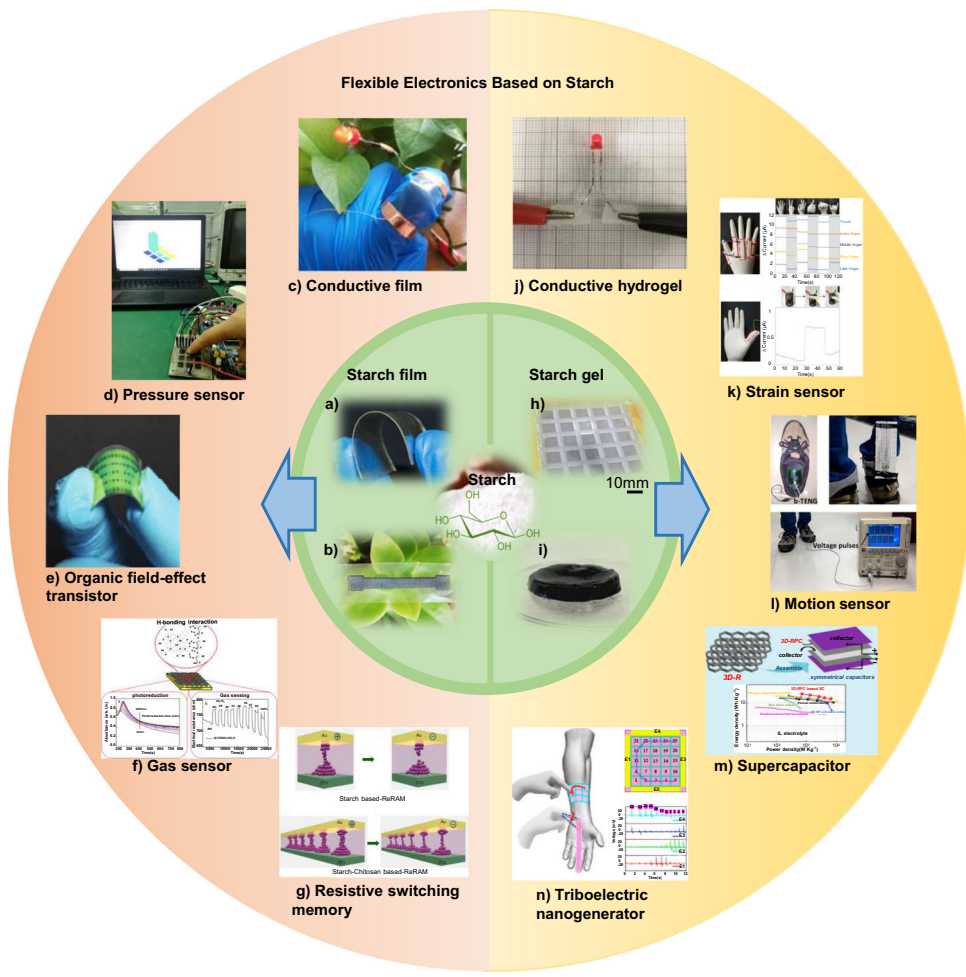


**Fig. 1 Summary of starch-based FEs.** Left, device on starch films: Starch film (**a**). Reproduced with permission<sup>86</sup>. Copyright 2019, Springer. Starch film (**b**). Reproduced with permission<sup>37</sup>. Copyright 2019, American Chemical Society. **c** Conductive film. Reproduced with permission<sup>38</sup>. Copyright 2018, American Chemical Society. **d** Pressure sensor. Reproduced with permission<sup>37</sup>. Copyright 2019, American Chemical Society. **e** Organic field-effect transistor. Reproduced with permission<sup>33</sup>. Copyright 2017, Wiley. **f** Gas sensor. Reproduced with permission<sup>98</sup>. Copyright 2020, American Chemical Society. **g** Resistive switching memory. Reproduced with permission<sup>35</sup>. Copyright 2016, American Chemical Society. Right, device on starch gels: Starch gel (**h**). Reproduced with permission<sup>39</sup>. Copyright 2018, American Chemical Society. Starch gel (**i**). reproduced with permission<sup>147</sup>. Copyright 2019, Elsevier. **j** Conductive hydrogel. Reproduced with permission<sup>45</sup>. Copyright 2019, American Chemical Society. **k** Strain sensor. Reproduced with permission<sup>151</sup>. Copyright 2019, Elsevier. **l** Motion sensor. Reproduced with permission<sup>40</sup>. Copyright 2019, American Chemical Society. **m** Supercapacitor. Reproduced with permission<sup>158</sup>. Copyright 2019, American Chemical Society. **n** Triboelectric nanogenerator. Reproduced with permission<sup>39</sup>. Copyright 2018, American Chemical Society.

other chemical modification<sup>50,51</sup>. Moreover, starch has outstanding environmental degradability and good biocompatibility. These characteristics make it an important candidate as raw material for fabricating green FEs.

Starch, is the most widely used biodegradable materials for now. In Europe, 50% of the produced starch was used for non-food applications<sup>52</sup>, such as the composition in adhesives and paper binders, textiles, chemical production, the feedstock for fermentation and other industrial products<sup>53</sup>. In addition, starch has physical, chemical, and functional properties, including good water solubility, gelatinization, high temperature adhesion behavior, and easy modification. The utilization of starch as a platform for building FEs at least has following advantages: (1) Starch is one of the most abundant renewable materials with extremely low cost. (2) Starch is degradable in water and soil without toxic residues thus being regarded as environmentally friendly materials. (3) Starch is biocompatible and suitable for implantable electronics. (4) Starch is easily transformed into flexible, foldable films and gels. (5) Starch is light in weight. Comparing with other biomass materials for FEs, the starch still has some advantage.

For instant, it shows better solubility than cellulose and it holds lower cost than proteins<sup>53,54</sup>.

## FES BASED ON STARCH FILMS

Starch is easy to be transformed into a film through heating in the presence of water followed by casting and drying. However, the starch films prepared by pure natural starch are usually fragile with low transparency. They are usually reinforced by compositing with other polymers, adding plasticizers, or modification through physical or chemical strategies<sup>38,55,56</sup>. The modified starch films may obtain acceptable mechanical property<sup>57,58</sup>, good flexibility<sup>49</sup>, or other features such as electrical conductivity<sup>59</sup>, making them more favorable to be utilized as soft substrates or the constituents of FEs. The data of FEs based on starch films were listed in Table 1.

### Conductive films derived from starch

Conductive films can be easily casted with starch when electroconductive materials are encapsulated. The most frequently used conducting components include graphene,

**Table 1.** Summary of FEs based on starch films.

Device Type	Materials	Performance	Function of starch	Ref
Conductive film	Starch, graphene	$9.7 \times 10^{-4} \text{ S cm}^{-1}$	Modification of graphene	48
Conductive film	Starch, SWCNT	$10^{-3} \text{ S cm}^{-1}$	Substrate	61
Conductive film	Starch nanocrystals, GO	$65.8 \mu\text{S m}^{-1}$	Dispersing agent	65
Conductive film	Starch, SCNT-PG-PEDOT	$46 \Omega \text{ sq}^{-1}$	Substrate	38
Conductive film	Starch, ionic liquid	$>10^{-3} \text{ S cm}^{-1}$	Substrate	59
Conductive film	Starch, graphene	$3.9 \times 10^{-4} \text{ S cm}^{-1}$	Filler	66
Conductive film	Mater-Bi, graphene	$\sim 10 \Omega \text{ sq}^{-1}$	Dispersing agent	70
Conductive film	Starch, AuNP	$<1.0 \Omega \text{ sq}^{-1}$	Reducing and stabilizing agents	71
Strain sensor	Starch, egg white, Ag	$<1.0 \Omega \text{ sq}^{-1}$	Substrate	86
Gas sensor	Starch, CNT	Sensitivity enhanced	Functionalization of CNT	97
Gas sensor	Potato starch, graphite flakes	10–1000 ppm	Functionalization of graphite	98
Chemical sensor	Starch, GO, AuNP	1.5 to 22 $\mu\text{mol L}^{-1}$	Substrate	87
Multifunctional sensor	Starch, porous carbon	Strain ( $GF = 134.2$ ), temperature (25–90°C), pressure (0–250 kPa)	Substrate	37
Supercapacitor	Starch, NaClO <sub>4</sub> , glutaraldehyde	ESW~2.4 V	Electrolyte	106
Supercapacitor	Starch, Ni quantum dots	Specific capacitance $1120 \text{ F g}^{-1}$	Assistant	107
Nanogenerator	Starch, lignin	Power density $173.5 \text{ nW cm}^{-2}$	Electrode	119
Nanogenerator	Starch	Output voltage 11.2 V	Electrode	120
Nanogenerator	Starch, cellulose	Output voltage 60–300 mV	Electrode	121
Nanogenerator	Starch	Output voltage 1.2 V	Electrode	122
Nanogenerator	PDMS, starch	Output voltage ~560 V	Electrode	40
Transistors	Starch, glycerol	On/off ratio $2.6 \times 10^6$	Ion-based gate dielectric	128
Organic transistor	Starch, PVA, Ag	On/off ratio $6.9 \times 10^4$ – $4.9 \times 10^5$	Substrate	33
Memristor	Starch, chitosan, Au, ITO	On/off current ratio $\sim 10^3$	Active layer	35
Electrolyte membranes	Starch, glycerol, ionic liquid, urea	Ionic conductivity $6.2 \times 10^{-4} \text{ S cm}^{-1}$	Proton exchange membrane	135

conducting polymers, ionic liquid, metals, and their alloys<sup>60</sup>. Zheng et al.<sup>48</sup> grafted starch molecules on the surface of graphene nanosheets (GN) in the presence of hydrazine hydrate. The conducting films were then fabricated with GN-starch filled plasticized starch, which shown conductivity up to  $9.7 \times 10^{-4} \text{ S cm}^{-1}$  when the content of GN-starch was only 1.774 wt%. The film also possessed excellent mechanical properties and moisture resistance, because the GN was well dispersed with the assistance of starch. Prusty et al.<sup>61</sup> prepared nanocomposites of functionalized single-walled carbon nanotubes (f-SWCNTs) and polyacrylonitrile-co-starch (PAN-co-starch) using in-situ polymerization technique. The nanocomposites have excellent electrical conductivity up to  $10^{-3} \text{ S cm}^{-1}$ .

The starch nanocrystals (SNCs) can be obtained after removing the amorphous zone by the treatment of enzyme, sulfuric acid, or hydrochloric acid<sup>62,63</sup>. The utilization of the starch nanocrystals to prepare composites may not only improve the mechanical properties of materials, but also increase the biodegradability<sup>63,64</sup>. Zhu and co-workers<sup>65</sup> extracted plate-like SNCs from natural waxy corns, which were then used to improve the dispersion of graphene in the composite film based on soybean protein (Fig. 2a). The composite conductive film shown a good conductivity of  $65.8 \mu\text{S m}^{-1}$ , enhanced mechanical strength, reduced water vapor and oxygen permeability as well as fine solvent resistance.

The conductive films with good transparency can also be prepared from starch. Miao and co-workers<sup>38</sup> spray-coated the carbon nanotube (CNT), pristine graphene (PG), and poly(3,4-ethylenedioxythiophene) (PEDOT) on the composite film of starch and chitosan to fabricate conducting film (Fig. 2b), which shown transmittance of 83.5% at 550 nm and low sheet resistance of  $46 \Omega \text{ sq}^{-1}$  as well as good mechanical performance. The conducting film worked as a transparent flexible electrode. Furthermore, it

can be rapidly degraded in lysozyme solution at room temperature indicated it is a green electronic device. Similar transparent film recently developed with graphene and potato starch, which achieved conductivity of  $3.9 \times 10^{-4} \text{ S cm}^{-1}$  with good moisture barrier properties<sup>66</sup>.

The most reported protocol to prepare starch films involved dissolving in water, gelatinizing and casting<sup>67,68</sup>. Plasticizers such as polyols (glycerol, ethylene glycol) or citric acid have to be added to reinforced the films<sup>49,55,69</sup>. Different from traditional-used plasticizers, ionic liquid (1-ethyl-3-methylimidazoliumacetate, [C<sub>2</sub>mim][OAc]) was employed as a functional plasticizer by Zhang and co-worker. to prepare electroconductive and transparent film (Fig. 2c)<sup>59</sup>. The film had good electrical conductivity ( $>10^{-3} \text{ S cm}^{-1}$ ) and was straightforwardly processed at moderate temperature (55–65 °C).

Except for solution casting as films, starch was used as a stabilizer in the preparation of conductive ink, which was then applied to fabricate conductive films. Cataldi et al.<sup>70</sup> dispersed commercial thermoplastic starch-based polymers (Mater-Bi, blends of thermoplastic starch and aliphatic polyester) and graphene nanosheets in an organic solvent to generate conductive inks, which was sprayed on pure cellulose substrate (Fig. 2d), and then hot pressed to form flexible conductive film (Fig. 2e). The sheet resistance reached as low as  $10 \Omega \text{ sq}^{-1}$  by regulating of the content of the graphene nanoplatelets. It was noted that the composite film maintained its mechanical and electroconductive performance even under many severe folding events, which is significant for flexible conductors. In the preparation of printable conductive ink, starch can also work as a reducing agent for metal ions. Bacalzo et al.<sup>71</sup> synthesized an aqueous gold nanoparticle (AuNP) ink suitable for inkjet printing using hydrolyzed starch as reducing agent and stabilizer (Fig. 2f). The AuNP ink can be

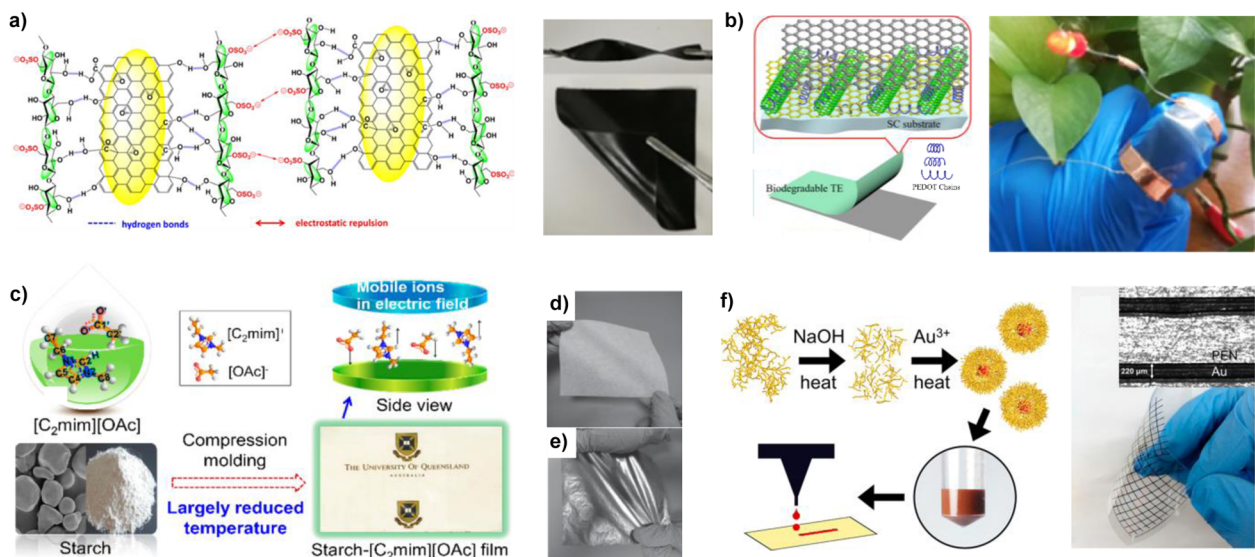


**Fig. 2 Conductive films derived from starch.** **a** Mechanism of the starch-aiding dispersion of graphene and a photograph of the corresponding conductive film. Reproduced with permission<sup>65</sup>. Copyright 2017, American Chemical Society. **b** Structural illustration and photograph of flexible conductive film with CNT-PG-PEDOT on starch and chitosan composite. Reproduced with permission<sup>38</sup>. Copyright 2018, American Chemical Society. **c** Starch-based conductive films prepared with ionic liquid as plasticizer. Reproduced with permission<sup>59</sup>. Copyright 2017, American Chemical Society. **d** Photograph of the porous cellulose fiber substrate and **e** the paper-like conductor after impregnating with inks of Mater-Bi starch-based polymer and graphene. Reproduced with permission<sup>70</sup>. Copyright 2015, Wiley. **f** Preparation process and image of the conductive film with inkjet printing of AuNP ink using starch as reduce agent. Reproduced with permission<sup>71</sup>. Copyright 2018, American Chemical Society.

printed and sintered at low temperature ( $<200^{\circ}\text{C}$ ) to generate conductive film with resistance as low as  $1.0\Omega\text{ sq}^{-1}$ . In this strategy, the starch solution was heated and hydrolyzed in NaOH solution, and then activated to reduce  $\text{Au}^{3+}$  in  $\text{HAuCl}_4$  solution to  $\text{Au}^0$ . Some starch molecules were hydrolyzed to stabilize the nanoparticles and control their further growth. This water-based ink can be used to print conductive patterns on a variety of substrates, demonstrating the versatile possibility of application in FE devices development.

### Sensing elements on starch films

Flexible sensing devices have important applications in the fields of human health monitoring, human-machine interface and wearable devices, which have attracted extensive attentions in recent year<sup>13,72,73</sup>. According to the application of detection, the sensing devices can be divided into physical sensors<sup>74–76</sup>, chemical sensors<sup>77–79</sup>, and biological sensors<sup>80–82</sup>. The starch have been used to develop degradable or recyclable flexible sensors because it is biocompatible and reproducible.

**Strain sensor.** Strain sensor is a device that transforms deformation into electrical signal, which is widely used in wearable devices<sup>75,83–85</sup>. Liu et al.<sup>86</sup> demonstrated a high-performance transparent strain sensor using starch to fabricate conductive matrix. The egg white was used as the sacrificial layer to support the conducting networks of silver by electro-plating. The starch solution was then dip-coated on the surface of the silver mesh and generated self-supported starch film with silver networks embedded (Fig. 3a), which shows low electro-resistivity ( $<1.0\Omega\text{ sq}^{-1}$ ) and high transparency (82%) (Fig. 3b). As shown in Fig. 3c, the resistance of the strain sensor changes following multiple bending cycles, which can be used to detect movements of human joints. The starch can be easily degraded and removed by water to yield an independent Ag network, indicating that the devices is recyclable.

**Chemical sensor.** Chemical sensors are used to detect chemicals in liquid or gas state, which have potentials in environment

monitoring, chemical diagnose, warning of hazardous gas. Jodar et al.<sup>87</sup> modified glassy carbon electrodes with RGO, gold nanoparticles (GNPs), and potato starch (PS) to produce a stable RGO-GNPS-PS conductive film as an electrochemical sensor for detection of estriol (Fig. 3d), which was a pollutant found in environment and aquatic organisms. The starch had good film-forming property and chemical stability, which was demonstrated in good supportability and permeability, as well as to compensate for the surface roughness of the electrode. The linear response of estriol was found in the range of  $1.5\text{--}22\mu\text{mol L}^{-1}$ , and the detection limit was  $0.48\mu\text{mol L}^{-1}$ . The RGO-GNPS-PS also effectively recycled 92.1–106% of estriol in natural water samples and synthetic urine. Similar strategies were used to fabricate electrochemical sensors for the detection of various chemicals<sup>88–92</sup>, in which the starch played an important role such as the substrates.

**Gas sensor.** The gas sensor is a device that detects various gas such as different organic vapors. It is also known as electronic nose<sup>79,93–95</sup>. Starch can be used to tune the nanostructure of gas sensor to enhance its sensitivity and selectivity<sup>96</sup>. Kumar et al.<sup>97</sup> investigated the use of amylose and amylopectin functionalized carbon nanotubes (CNT) to fabricate electronic noses on micro-electrodes by spraying them layer by layer to detect vapors of water, methanol and toluene. As shown in Fig. 4a, they adsorbed on the surface of carbon nanotubes in helical or random conformation, respectively, which changed the junction gap of CNT. Interestingly, amylose increased the sensitivity of the CNT sensor to water, while amylopectin increased the sensitivity to toluene (Fig. 4b). In another example, Peregrino et al.<sup>98</sup> prepared gas sensor by assembling starch and graphene oxide (GO) layer by layer on a quartz substrate (Fig. 4c). They found at least three important roles that the starch was played. At first, hydrogen bondings were established between  $-\text{OH}$  groups in starch and  $-\text{C}-\text{O}-\text{C}-$ , and  $=\text{C}=\text{O}$  from GO, which improved the efficiency of film assembling. Secondly, the starch provided additional electron density during photoreduction of GO, making the reduction faster and more efficient. Thirdly, the sensitivity of the device to humidity was improved since the starch is hygroscopic.

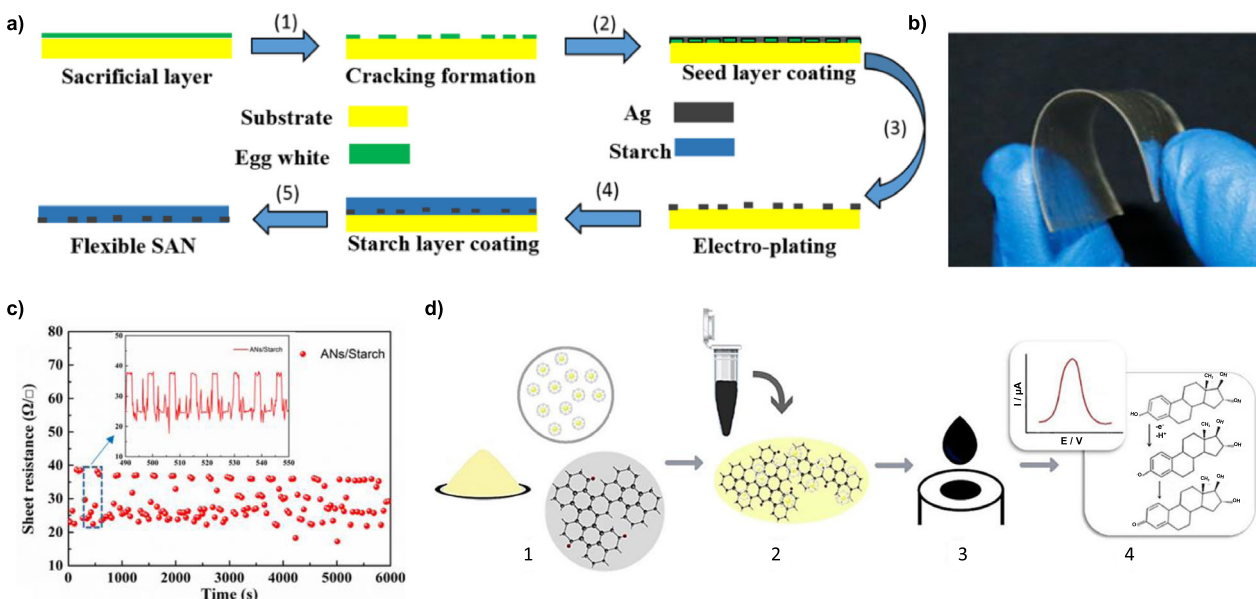


**Fig. 3** Flexible strain and chemical sensors based on starch films. **a** Fabrication processes and **b** flexibility demonstration as well as **c** sheet resistance corresponding to bending times of a sensor based on starch-Ag networks (SANs). Reproduced with permission<sup>86</sup>. Copyright 2019, Springer. **d** Preparation protocol of the chemical sensor that detects estriol from RGO-GNPs-PS. Reproduced with permission<sup>87</sup>. Copyright 2017, Springer.

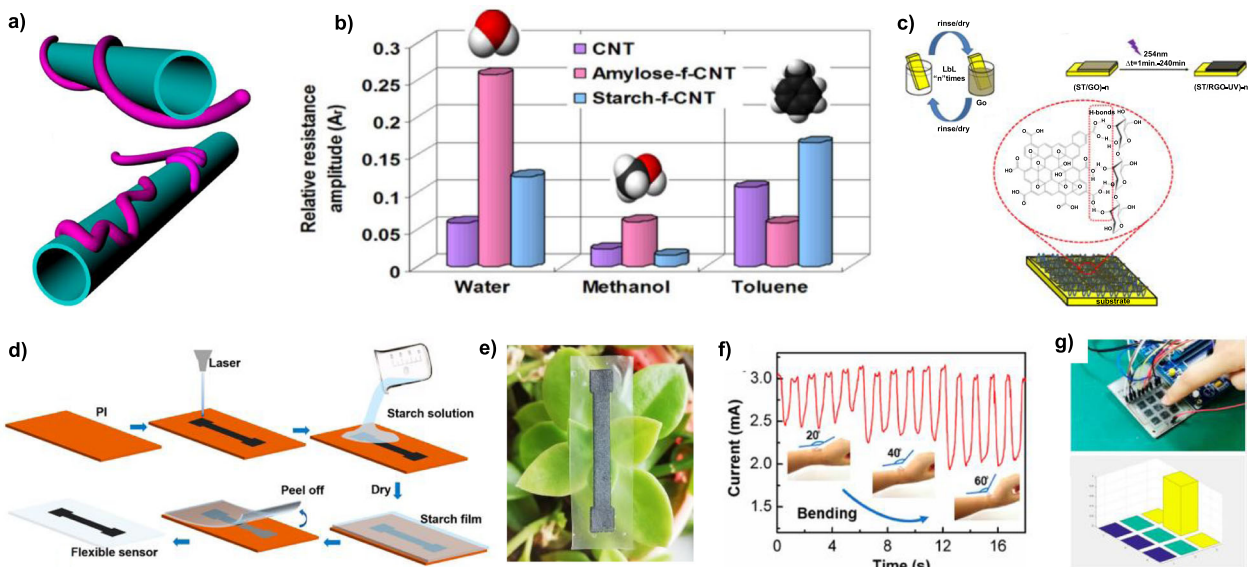


**Fig. 4** Flexible gas and multifunctional sensors based on starch films. **a** Possible conformation of amylose-f-CNT and starch-f-CNT sensors and **b** their selectivity for different vapors. Reproduced with permission<sup>97</sup>. Copyright 2012, Elsevier. **c** Illustration of the layer-by-layer (LbL) deposition, photochemical reduction, and hydrogen bonding of the starch-GO sensor on quartz substrate. Reproduced with permission<sup>98</sup>. Copyright 2020, American Chemical Society. **d** The preparation procedure and **e** photograph of a multimodal flexible sensor on starch film. **f** Real-time current signal for monitoring of wrist bending with different angles. **g** The sensor matrix for detection of spatial pressure. Reproduced with permission<sup>37</sup>. Copyright 2020, American Chemical Society.

Therefore, it is convincing that the starch may find more applications in fabricating such intelligent device.

**Multifunctional sensor.** The preparation of FEs with low cost and high precision detection of various stimuli are the significant challenges<sup>12,99,100</sup>. In our previous work<sup>37</sup>, laser-induced porous carbon was transferred to the starch film producing a flexible multimodal sensor (Fig. 4d, e). The strain, humidity, temperature, and pressure can be detected with one device, thus decreasing the price of sensor matrix. The sensor can detect strain with gauge factor (GF) of 134.2, response time of approximately 130 ms, and

good durability more than 1000 cycles of bending-unbending, which can be used to monitor human motions including bending of fingers, wrists and knees (Fig. 4f) and pressure (Fig. 4g). Furthermore, multiple stimuli can be distinguished with the sensor, such as pressure coupled with temperature change. More importantly, the sensor can be degraded in water thus being free of e-waste, so it is a typical green electronic device.

## Supercapacitor on starch films

Traditional energy sources cannot fulfill the dramatical increment of energy demands in nowadays, thus the alternate and renewable energy source attracted widely attentions. The electrolyte is one of the most important parts of renewable energy device. Polymers including polyethylene oxide (PEO), poly (vinylidene fluoride) (PVDF), and poly (methylmethacrylate) (PMMA) were intensively investigated as host of salt complex electrolytes in previous research<sup>101–105</sup>. Recently, people found the starch can meet the 3Es requirement of electrolytes that are (a) environment friendly, (b) economical and (c) easy to mould in desired shape and size. For instance, Chauhan et al.<sup>106</sup> prepared a highly transparent film with conductivity up to  $10^{-2}$  S cm<sup>-1</sup> using composite of corn starch and NaClO<sub>4</sub> after cross-linking with glutaraldehyde. The equivalent series resistance of the sample with thickness of 0.8 mm was  $\sim 6.252$  Ω, the electrochemical stability window (ESW) was  $\sim 2.4$  V and the ion relaxation time was  $\sim 65$  μs. Chen and co-workers<sup>107</sup> synthesized ultrathin carbon nanosheet-supported Ni quantum dot hybrids (C-Ni-QDs) through hydrothermal method followed by annealing process with the assistance of starch. The C-Ni-QDs was used to assemble a supercapacitor, which shown a high specific capacitance up to  $1120$  F g<sup>-1</sup> at  $2$  A g<sup>-1</sup> and a capacitance retention of 97% after 2000 cycles. These results shown that the starch is a promising carbon sources for supercapacitors that is inexpensive and abundant.

## Nanogenerator on starch films

Nanogenerators based on triboelectric, piezoelectric, and electrostatic induction effects have been proposed to construct self-actuating systems that produce electricity from various mechanical energies, including human motion<sup>108–110</sup>, vibration, and wind<sup>111,112</sup>. The flexible nanogenerators can provide a flexible and portable energy collection system or work as self-powered sensors, which has recently become a hot research topic<sup>9,113–116</sup>.

Triboelectric nanogenerators (TENGs) are made of two materials with different triboelectric properties. The friction between the two films generate equal but opposite charges on both sides due to nanoscale surface roughness, while the friction potential layer generated in the interface region drives the flow of electrons in the external load<sup>117,118</sup>. Bao et al.<sup>119</sup> developed TENGs based on lignin-starch nanocomposites (Fig. 5a), in which the starch improved the uniformity of the film. When the ratio of lignin to starch in the composite film was 3:7, the highest output was reached. The average short-circuit current was  $3.96$  nA cm<sup>-2</sup>, and the open-circuit voltage was  $1.04$  V cm<sup>-2</sup>. Zhu et al.<sup>120</sup> assembled TENGs based on a starch film, using the coupling effect between human skin and starch film to develop a self-powered sensor for detecting human perspiration (Fig. 5b). Vela and co-workers<sup>121</sup> described a starch-cellulose-based TENG using potato starch, and sandpaper as the substrate of microstructure. They found that the output voltage depended on the thickness (50–200 μm) of the film. The electric output of 4 cm<sup>2</sup> TENG reached up to 300 mV in the presence of the starch film. Further research by Vela prepared a low-cost TENG using a starch film with micro-structure as a triboelectric dielectric layer (Fig. 5c)<sup>122</sup>. The 0.5% of CaCl<sub>2</sub> was added into the film to improve the voltage output from 0.4 to 1.2 V. Sarkar and co-workers<sup>40</sup> developed TENGs using thermoplastic starch film as a positive electrode and PDMS as negative electrode (Fig. 5d). This bilayer TENG (b-TENG) can generated open-circuit output voltage up to  $\sim 560$  V and output current density of around  $\sim 120$  mA m<sup>-2</sup>, which can light more than 100 LEDs. In addition, the TENG device can work as a self-powered pedometer for walking and a gait analysis sensor for health evaluation (Fig. 5e, f). The good performance of the devices benefited from the surface morphology of the starch film, which

may open a window for the low cost and environmental-friendly self-powered electronic devices.

## Organic transistor on starch films

Flexible organic field-effect transistor (OFET) devices have attracted much attention as a display technology<sup>123–127</sup>. Intrinsically flexible OFET has significant advantages compared with inorganic thin film transistors on accelerate technology update, simple production process and low cost. Shao et al.<sup>128</sup> used starch as an ion-base gate dielectric for oxide thin film transistors (Fig. 6a). It was found that the transistor performance is closely related to the specific capacitance and ionic conductivity of starch (Fig. 6b). Higher on/off ratio and field mobility can be achieved by glycerol incorporated starch. The results demonstrated the potential application of starch in thin film transistors. In Jeong's work<sup>33</sup>, a flexible OFET was fabricated on starch-PVA film by a vapor-deposited method (Fig. 6c). The starch film has good transparency (Fig. 6d), remarkable mechanical strength, and good stability in non-polar solvent. The calculated field-effect mobility was  $0.013\text{--}0.37$  cm<sup>2</sup> (Vs)<sup>-1</sup> with on/off ratio of  $6.9 \times 10^4\text{--}4.9 \times 10^5$  (Fig. 6e), which were comparable to that of other flexible OFETs. Interestingly, the device on the film can be quickly degraded in fishbowl water by the fungi inside, suggesting it is eco-friendly biodegradable FEs with low cost.

## Other electronics on starch films

Resistive switching memories (ReRAMs) are the major candidates for replacement of the state-of-the-art memory devices in the future due to their good scalability, ultrafast write and read access, and low power consumption<sup>129</sup>. The ReRAM using polymer as the active layer has the advantages of good flexibility, low cost, good processability and fine compatibility with various substrate. Biopolymers such as chitosan<sup>130</sup> and cellulose<sup>131</sup> have been considered in the electronic devices of synapses<sup>28,131,132</sup>. Due to the presence of loosely bound water molecules in the crystal network, the potato starch has reasonable ionic conductivity<sup>133,134</sup>. Raeis-Hosseini et al.<sup>35</sup> demonstrated a non-volatile, flexible and transparent ReRAMs device using potato starch and chitosan as active layer (Fig. 7a). The device was prepared with Au/starch-chitosan/ITO on PET flexible substrate by spin coating and thermal evaporation. The inset images in Fig. 7a shows a magnified optical image of the storage array on the flexible substrate. The resistance behavior of the device can be controlled effectively by the content of starch and chitosan as well as the chemical composition of starch (amylose and amylopectin). Both Au/starch/ITO/PET and Au/starch-chitosan/ITO/PET device shown good set/reset performance (Fig. 7b, c). Furthermore, the progressive setting/resetting behavior of this storage devices makes them potential in the application of neuromorphic devices such as simulation-based synaptic electronics.

Fuel cells and redox flow batteries provide considerable energy and power density that are more sustainable alternatives to lithium batteries. However, the perfluorosulfonic acid copolymer proton exchange membranes in these cells are still an important environmental problem. In Alday's work<sup>135</sup>, biopolymer electrolyte membranes (Bio-PEMs) were synthesized from starch, cellulose, and chitosan. The starch-based Bio-PEMs were doped with ionic liquid, glycerol, or urea (Fig. 7d), which reached the highest ionic conductivity of  $6.2 \times 10^{-4}$  S cm<sup>-1</sup> through a symmetrical cell test (Fig. 7e). These Bio-PEMs are promising alternatives for conventional copolymer membranes in sustainable electrochemical systems and biodegradable devices.

## FES BASED ON STARCH GELS

Gels derived from biopolymers have attracted increasing attentions as a result of their good biocompatibility, innate

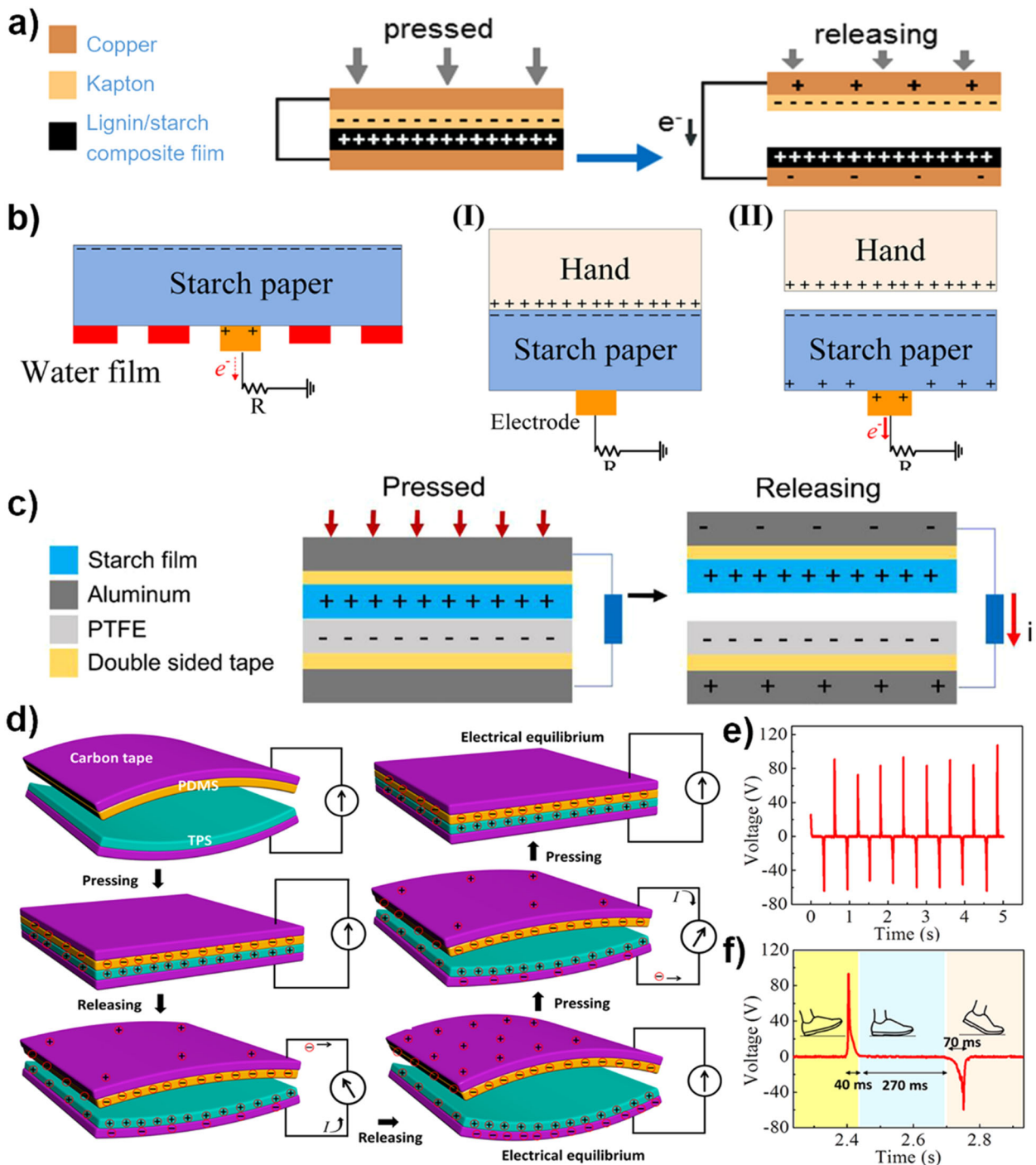


**Fig. 5 TENGs based on starch films.** **a** Mechanism of lignin-starch nanocomposite TENG. Reproduced with permission<sup>119</sup>. Copyright 2017, American Institute of Physics. **b** Mechanism of the starch paper-based TENG. Reproduced with permission. Reproduced with permission<sup>120</sup>. Copyright 2018, Springer. **c** Mechanism of TENGs based on  $\text{CaCl}_2$  modified starch film. Reproduced with permission<sup>122</sup>. Copyright 2019, Elsevier. **d** Schematic representation of structure and the working principle of TENGs from thermoplastic starch-PDMS and the corresponding outputs for **e** human walking detection and **f** gait analysis. Reproduced with permission<sup>40</sup>. Copyright 2011, American Chemical Society.

biodegradability, and crucial biological functions<sup>136–138</sup>. Niu et al.<sup>139</sup> reported a gelatin/ poly (acrylic acid N-hydroxysuccinimide ester) (PAA NHS ester)-based ionic conductive organohydrogel by introducing a glycerol/water binary solvent system, which was used as wearable health monitoring device. The starch was also widely used in the preparation of gels can readily generate a three-dimensional network via physical entanglement of amylose and/or amylopectin<sup>140</sup>. A large amounts of water or biological

fluids can be retained due to their good hydrophilicity. Furthermore, the starch chains may be easily cross-linked through the abundant hydroxyl groups. So, the starch-based gels were intensively investigated and shown great potential especially in biomedicine<sup>62,141–146</sup>. Gonzalez et al.<sup>147</sup> prepared starch-based hydrogels through the Diels-Alder cross-linking reaction between furan modified starch and water-soluble bismaleimide. The photograph and SEM images were shown in Fig. 8a. Graphene

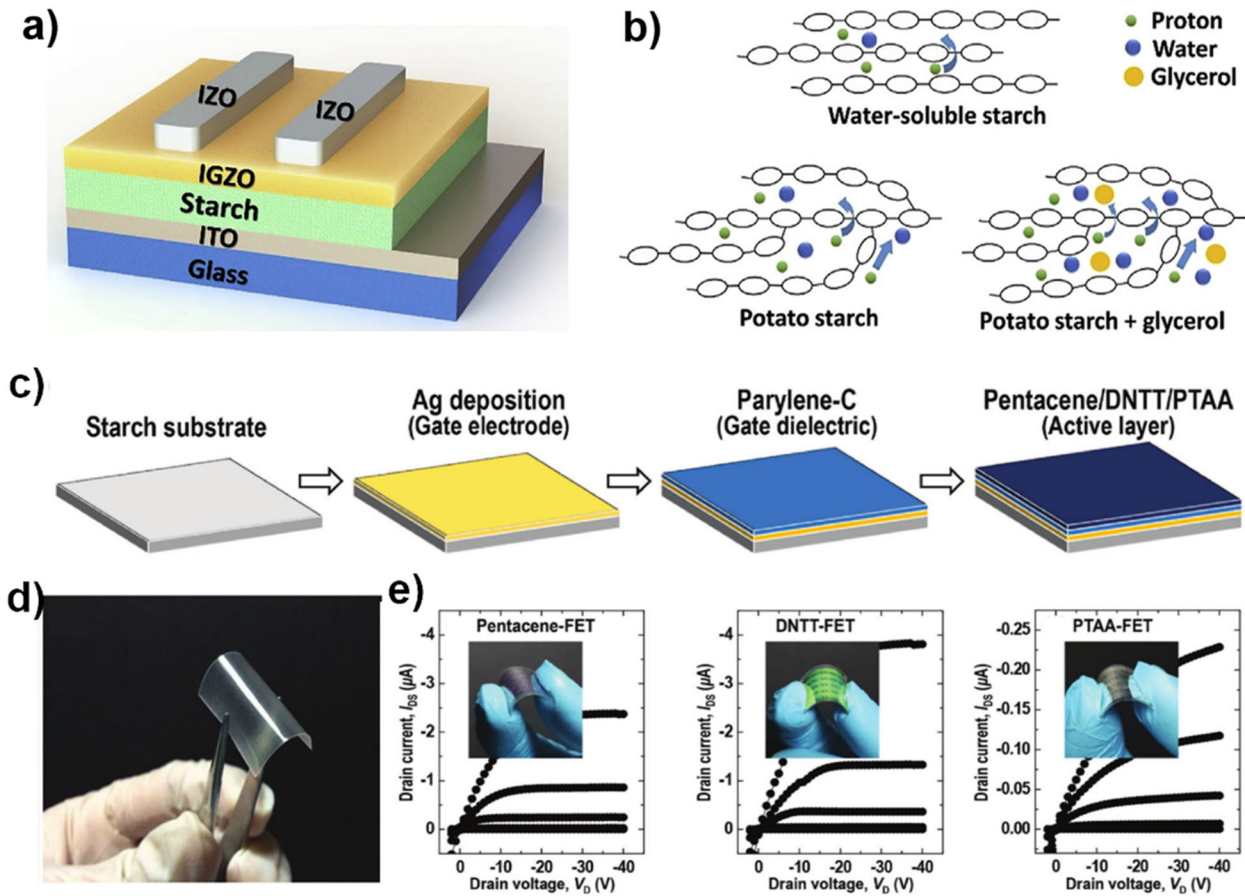


**Fig. 6** Organic transistor based on starch films. **a** Device structure of the thin film transistors with starch as the ion-based gate dielectric. **b** Schematic illustration of the proposed ion (proton) transportation in the starch-based gate dielectrics. Reproduced with permission<sup>128</sup>. Copyright 2017, Elsevier. **c** Schematic diagrams of fabrication process of the OFET based on starch-PVA film. **d** Photograph of the flexible starch-PVA film. **e** Output characteristics of various flexible devices fabricated on the starch-PVA film. The inset images in (e) show the fabricated devices and their flexible features. Reproduced with permission<sup>92</sup>. Copyright 2018, Wiley.

nano-particles were introduced to endow the antibacterial and electrical conducting property to the hydrogel, which might find prospects in biomedical application. Recently, Lin et al.<sup>146</sup> prepared an adhesive hydrogel from ionically crosslinked starch, which had good electrical conductivity, high tissue adhesion, strong antibacterial ability. The wound condition diagnosis and management might be realized due to the conductivity of the hydrogel considering the wound condition can be transferred into electrical outputs. In addition, the application of starch-based gels in smart window was also explored<sup>148</sup>. Wang et al. prepared smart window using thermosensitive starch gel as active layer, which shown an excellent solar modulation property of 17.9% and average light transmittance of 57.8%. The details of the reported FEs based on starch gels were listed in Table 2.

### Sensing elements based on starch gels

Various sensors were fabricated on starch gels to obtain biocompatible devices<sup>149,150</sup>. Kanaan et al.<sup>45</sup> synthesized a biodegradable semi-interpenetrating polymer networks (S-IPNs) based on starch and copolymer of 2-hydroxyethyl methacrylate (HEMA) and 1-butyl-3-metaprazor-lium chloride (BViMCl) cationic (Fig. 8b). According to the relative composition of different monomers, the electronic and ionic conductivity of the hydrogel was manipulated in range from 0.1 to 5.2 S cm<sup>-1</sup>, and the complex shear modulus was regulated in a range from 0.6 to 6.4 MPa. The flexible hydrogel worked as a multi-stimuli-responsive platform that was sensitive to changes of

relative humidity, ionic strength and current. Therefore, the adsorption/release capacity of the hydrogel toward L-tryptophan was regulated through the DC voltage applied. Furthermore, the hydrogel shown good biocompatibility due to the existence of starch. It may find widely applications in biological separation, sewage treatment systems, biomedical and electrochemical equipment. Liu et al.<sup>151</sup> developed a flexible, ultra-low-cost conductive hybrid elastomer by mixing polydimethylsiloxane (PDMS) and starch hydrogel, which had strong elasticity (56 kPa) and acceptable conductivity ( $10^{-2}$  S m<sup>-1</sup>). The composite elastomer can detect stress (gauge factor 0.71), strain (gauge factor 2.22) and humidity (sensitivity of  $1.2 \times 10^{-6}$  S m<sup>-1</sup> RH %<sup>-1</sup>). Moreover, the sensor can be used for monitoring finger movements and bottle grasping (Fig. 8c, d), demonstrating its potential in artificial skin and wearable devices. Noticeably, the volume ratio of the starch and PDMS in the composite was about 3:1, which is also significant for the cost reduction. Xu et al.<sup>152</sup> selected potato starch as the main network and introduced polyvinyl alcohol (PVA) and borax to improve the mechanical and conductive properties of hydrogels. Due to the dual reversible interactions of hydrogen bonding and the boronic ester linkages, the hydrogels shown enhanced mechanical performance and super-fast self-healing ability. The hydrogel was used as a strain sensor with GF = 1.02 at 110–200% strains, which can quickly perceive human movements with a response time of 180 ms, even small movements such as swallows and sounds.

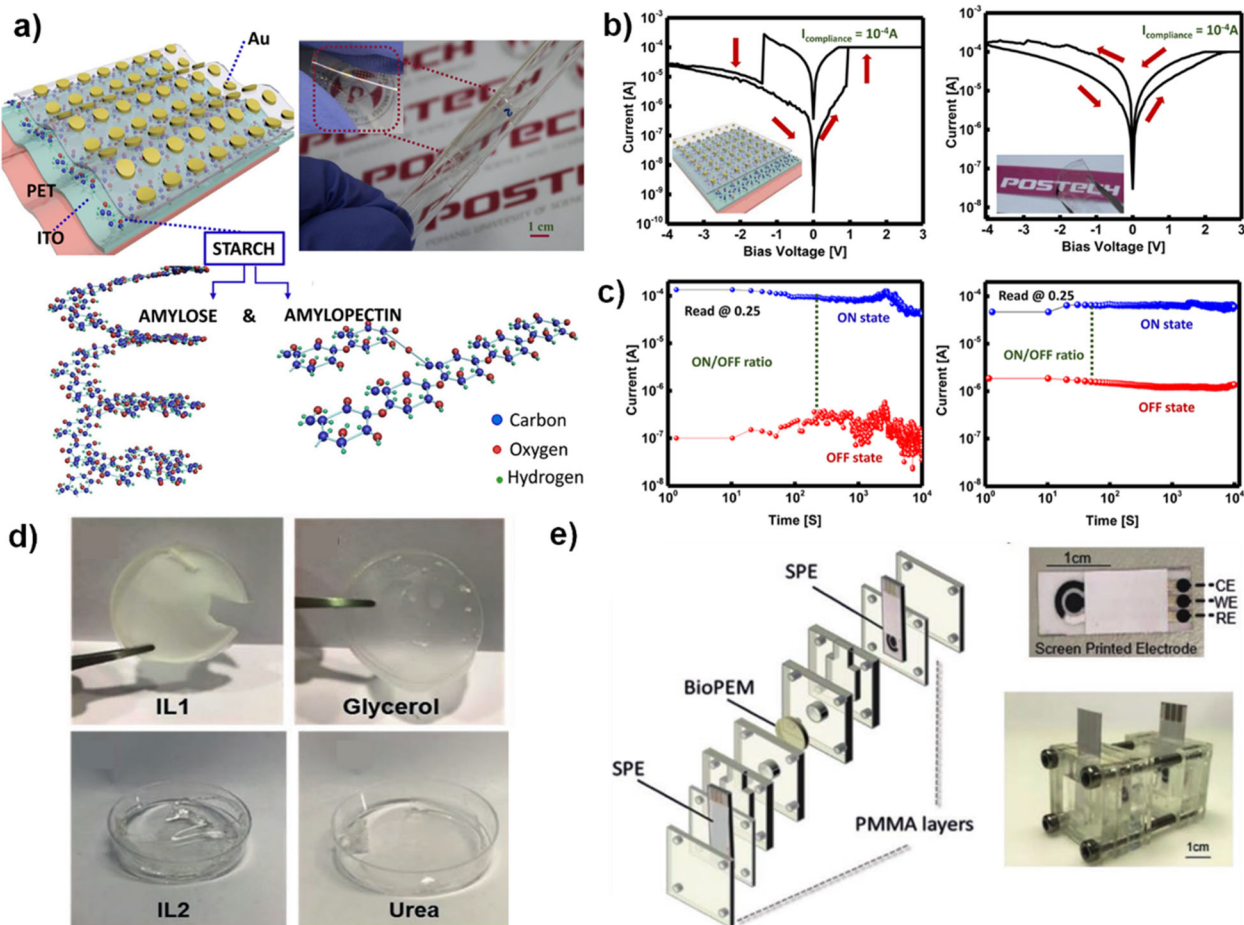


**Fig. 7** Memory devices and batteries based on starch films. **a** Schematic illustration of the structure and the photograph of flexible ReRAM memory device on starch-chitosan. **b** I-V curves and **c** on/off ratio of the ReRAM devices composed of Au/starch/ITO/PET and Au/starch-chitosan/ITO/PET. Reproduced with permission<sup>35</sup>. Copyright 2016, American Chemical Society. **d** Photographs of the starch based BioPEMs and **e** the corresponding battery cell. Reproduced with permission<sup>135</sup>. Copyright 2020, Wiley.

The amylose and amylopectin may exhibit different mechanical property due to their structure difference. The linear chain of amylose makes it more resistant to processing and may show better mechanical performance and less water sensitivity<sup>150</sup>. Liu et al.<sup>153</sup> prepared flexible, transparent, ionically conductive hydrogel by simply mixing high-amylose starch with CaCl<sub>2</sub> solution. This material shown adjustable mechanical strength (500–1300 kPa), elongation at break (15–32%), Young's modulus (4–9 MPa), toughness (0.05–0.26 MJ/m<sup>3</sup>) and suitable resistivity (3.7–9.2 Ω·m). The hydrogel can be used as a sensor to detect strain, moisture and liquid with different pH value. The Amylopectin with dendritic structure may supply more physical interaction with other materials thus is suitable to fabricate adhesive hydrogel. Gao et al.<sup>154</sup> combined amylopectin with poly(acrylamide-acrylic acid) (P(AAm-AAc)) to prepare a hydrogel with good adhesion, toughness and electrical conductivity. As a wearable sensor, the hydrogel shown high strain sensitivity (GF = 6.93) and stability, which was used to monitor various motions of human, such as joint bending, walking, jumping, even talking.

#### Supercapacitor based on starch gels

Due to the carbon-rich nature and low price, starch has been used as a common precursor for producing activated carbons which have wide applications such as electrode material<sup>155–157</sup>. Wang et al.<sup>34</sup> reported a simple, rapid and scalable method for the production of the three-dimensional flexible and porous graphene

electrode materials, which simply dissolved starch in GO suspension followed by thermal carbonization and chemical activation. The electrode had a high specific surface area of 1,519 m<sup>2</sup> g<sup>-1</sup>, high energy density of 19.8 Wh kg<sup>-1</sup> at the power density of 0.5 kW kg<sup>-1</sup> and a high power density of 9.9 kW kg<sup>-1</sup> at the energy density of 9.6 Wh kg<sup>-1</sup>. The structural diagram and energy storage performance of the supercapacitor are shown in Fig. 9a. Furthermore, the flexible supercapacitors kept specific capacitance retention rate of 80% after 8000 cycles at 10 A g<sup>-1</sup>. The supercapacitor worked well even under large angle bending (138°), thus may find potential in the application of wearable equipment. Similarly, Liu et al.<sup>158</sup> prepared three-dimensional interconnected reticular porous carbon electrode using corn starch as the carbon precursor (see protocol in Fig. 9b). The 3D electrode shown high specific capacitance of 372 F g<sup>-1</sup> at a current density of 0.5 A g<sup>-1</sup> in 2 M KOH electrolyte with high energy density and long cycle life. The cyclic C–V diagram is shown in Fig. 9c. Considering the high purity and low cost of corn starch and the excellent capacitance performance of 3D electrode, this study opens a way for the large-scale production of low-cost and high purity porous carbon for supercapacitors. Willfahrt et al.<sup>159</sup> prepared a screen printable hydrogel as electrolyte using corn starch and citric acid with ionic conductivity up to  $2.30 \pm 0.07 \text{ mS cm}^{-1}$ . The hydrogel shown excellent printability and prolonged stability against degradation. The specific capacitance of the printed supercapacitor was up to 54 F g<sup>-1</sup>.

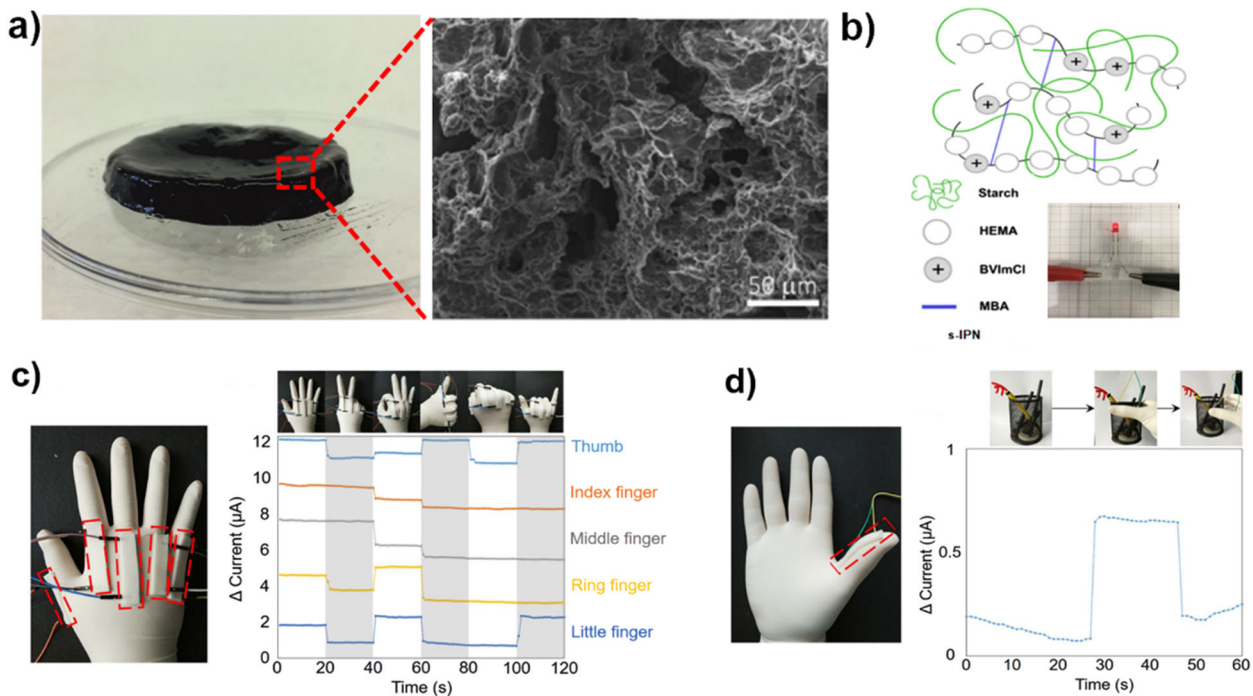


**Fig. 8 Conducting and sensing elements based on starch gels.** **a** Photograph and SEM images of the starch/graphene hydrogels. Reproduced with permission<sup>147</sup>. Copyright 2018, Elsevier. **b** Chemical structure of the S-IPNs hydrogel with electronic and ionic conductivity. Reproduced with permission<sup>45</sup>. Copyright 2019, American Chemical Society. **c** Photographs of starch hydrogel sensors on the glove and the responding current signal under different hand configurations; **d** photographs and signal of starch hydrogel sensor to monitor the hand grasping a pencil vase. Reproduced with permission<sup>151</sup>. Copyright 2019, Elsevier.

**Table 2.** Summary of FEs based on starch gels.

Device Type	Materials	Performance	Function of starch	Ref
Sensor/biomolecules carrier	Starch, poly (HEMA-co-BVIImCl)	Electric responsive 2–5 V	Increase biocompatibility	<a href="#">45</a>
Adhesive hydrogel	Starch, cross linkers	Viscoelastic antibacterial conductivity	Adhesives	<a href="#">146</a>
Smart window systems	Starch, AgNWs, cellulose	Solar modulation 17.9%	Active layer	<a href="#">148</a>
Sensor	Starch, PDMS	Stress (GF = 0.71), strain (GF = 2.22), humidity ( $1.2 \times 10^{-6} \text{ S m}^{-1} \text{ RH}^{-1}$ )	Substrate	<a href="#">151</a>
Sensor	Starch, PVA, borax	Strain (GF = 1.02), S = 180 ms	Network structure	<a href="#">152</a>
Sensor	Starch, CaCl <sub>2</sub>	Strain, moisture, pH	Network structure	<a href="#">153</a>
Sensor	Amy, P(AAm-AAc)	Strain (GF = 6.93)	Assistant	<a href="#">154</a>
Supercapacitor	Starch, GO	Energy density 19.8 Wh kg <sup>-1</sup>	Carbon precursor	<a href="#">34</a>
Supercapacitor	Starch, KOH	Energy density 24.5 Wh kg <sup>-1</sup>	Carbon precursor	<a href="#">158</a>
Supercapacitor	Starch, citric acid	Specific capacitance 54 F g <sup>-1</sup>	Electrolyte	<a href="#">159</a>
Supercapacitor/absorbent	Starch, GO	Specific capacitance 316 F g <sup>-1</sup>	Modification of GO	<a href="#">41</a>
Triboelectric nanogenerator	Starch, PDMS, silicone rubber	Open-circuit voltage ~25 V	Electrode	<a href="#">39</a>

Starch-based nanoparticle was also used in the preparation of supercapacitors. For example, starch nanocrystals prepared by hydrolysis of starch have been widely used in many fields<sup>62,63,65,160</sup>. Chen et al.<sup>41</sup> used graphene oxide (GO) nanosheets to combine with dialdehyde starch nanocrystals to fabricate porous, strong, compressible aerogels that were used as supercapacitor electrodes and highly efficient adsorbents (Fig. 9d). The starch nanocrystal prevented self-stacking between graphene nanopores to improve the electrical properties of aerogels, resulting in the increment of the specific capacitance from 198 to 316 F g<sup>-1</sup>. The good mechanical properties and high specific surface area of the aerogels promised their application in dyes removing. Therefore, the hybrid aerogel might be used as a

flexible electrode of supercapacitors or candidate materials for biomedical and environmental cleaning.

### Nanogenerator based on starch gels

A common limitation of the sensing system is that the most sensors cannot work without external power source. TENGs can act as an active sensor to detect pressure without the use of an external power source<sup>9,110,111</sup>. In addition, complex circuits can also be avoided in these self-powered devices. Chen et al.<sup>39</sup> proposed a self-powered, flexible, triboelectric sensor (SFTS) composed of starch-based hydrogel, polydimethylsiloxane (PDMS) and silicone rubber. The two-dimensional SFTS (2D-SFTS) with a

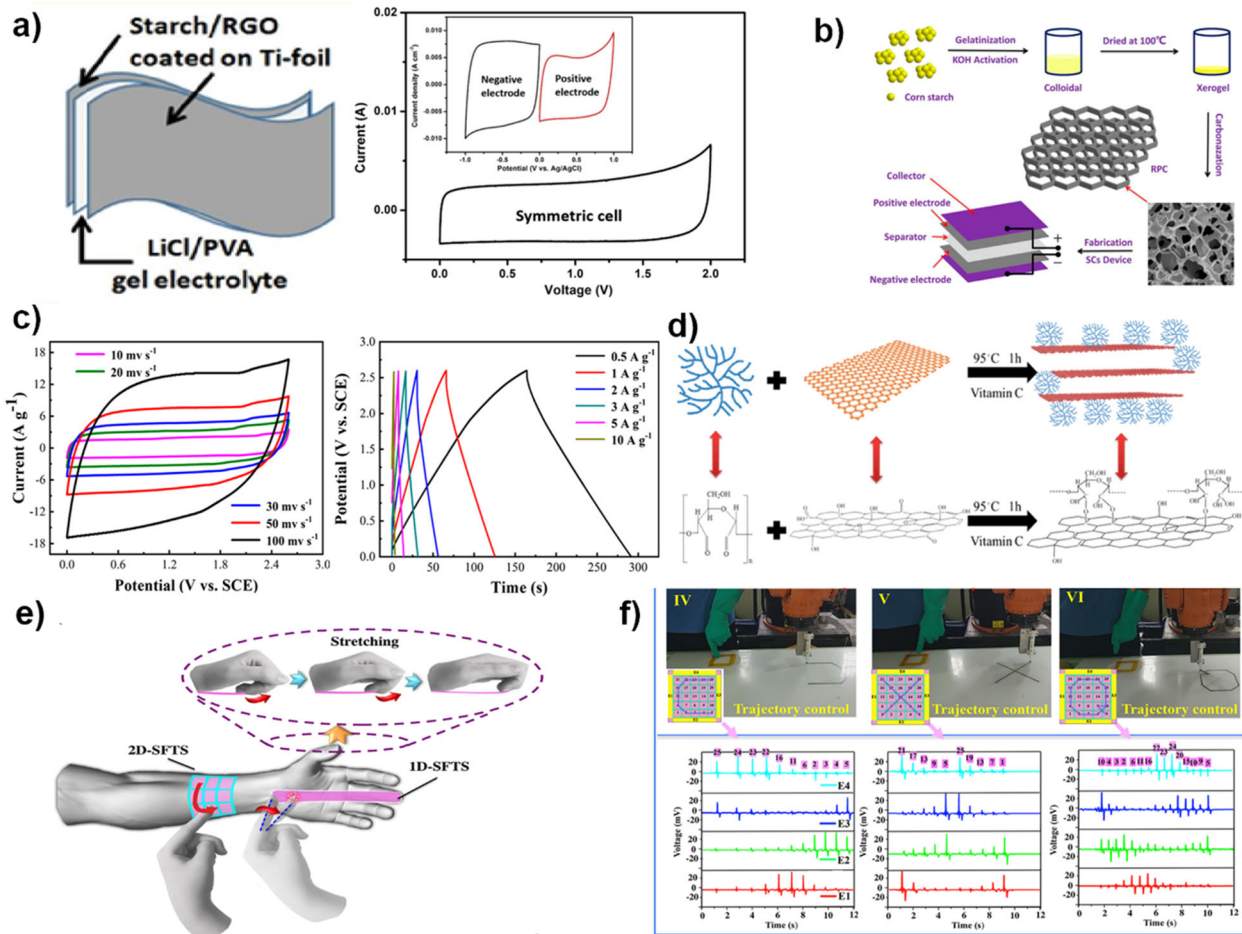


**Fig. 9 Supercapacitor and nano generator based on starch gels.** **a** Schematic diagram of supercapacitor and capacitive performances of starch/RGO and starch/RGO supercapacitor. Reproduced with permission<sup>34</sup>. Copyright 2017, American Chemical Society. **b** Schematic diagram and **c** electrochemical performances of the supercapacitor with a 3D printed electrode. Reproduced with permission<sup>158</sup>. Copyright 2019, American Chemical Society. **d** Aerogel made of GO and starch nanocrystal that can be used as supercapacitor electrodes and highly efficient adsorbents. Reproduced with permission<sup>41</sup>. Copyright 2019, American Chemical Society. Self-powered, flexible, triboelectric sensor (SFTS) for **e** 3D motion detection and **f** 3D robotic manipulations. Reproduced with permission<sup>39</sup>. Copyright 2018, American Chemical Society.

grid structure can track continuous sliding information on the fingertip, such as trajectory, velocity, and acceleration. 3D motion detection (Figs. 9e) and 3D robotic manipulation (Fig. 9f) were also realized by combining with a one-dimensional (1D) SFTS. By introducing starch, the cost was decreased and environmental friendliness was improved for the composite elastomer.

## DEGRADABILITY AND BIOMATERIALS OF STARCH-BASED ELECTRONICS

The natural polymers including cellulose, lignin and starch belong to biodegradable polymer materials, which can be degraded by bacteria, mold, algae, and other microorganisms through enzyme or chemical hydrolysis. The main molecular chains are firstly broken resulting into the reduction of molecular weight. They eventually decomposed to small molecules or metabolized into carbon dioxide and water<sup>161</sup>. The polymers with higher molecular weight may take a longer time to be degraded. A greater microbial diversity may also accelerate the degradation, such as the activated sludge.

The natural polymers such as starches usually have to be blended with synthetic polymers to reach the mechanical requirements in practical application. The degradation of the composite of starch and synthetic polymers may be accelerated because the starch might be firstly decomposed by

microorganisms, which makes the hybrids porous and increases the specific surface area, thus facilitating further enzymatic hydrolysis or decomposition in the nature<sup>162</sup>.

As known the starch is derived from nature and should be degradable, lots of experimental protocols have been established to confirm the degradation of FEs based no starch. One intuitive way is recording the decomposing process of the device. For instance, the conductive starch film developed by Miao and co-workers<sup>38</sup> was found to be quickly dissolved and disappeared in the buffer of acetic acid and sodium acetate ( $\text{pH} = 4.5$ ) with 3wt % lysozyme after about 8 min, as shown in Fig. 10a. In another example, the starch device was gradually covered with fungus until it was completely degraded when it was soaked in fish tank water (Fig. 10b)<sup>33</sup>. In our previous work, the starch-based sensor was broken in the flush water generated by the shower nozzle and then completely decomposed in about 10 min, indicating a rapid degradation under water flushing (Fig. 10c)<sup>37</sup>. Besides, the starch-based devices were also demonstrated to be degradable in static water<sup>37,120</sup>. It should be pointed out that the treatment of the other materials in these devices were usually ignored, including the graphene, conducting polymers, or metals. The reason may be ascribed to their non-hazardous feature and low content of these conductive materials in FEs. However, it may be a risk when the usage of the starch-based FEs is large enough. The non-degradable components may be recycled by filtration or flotation

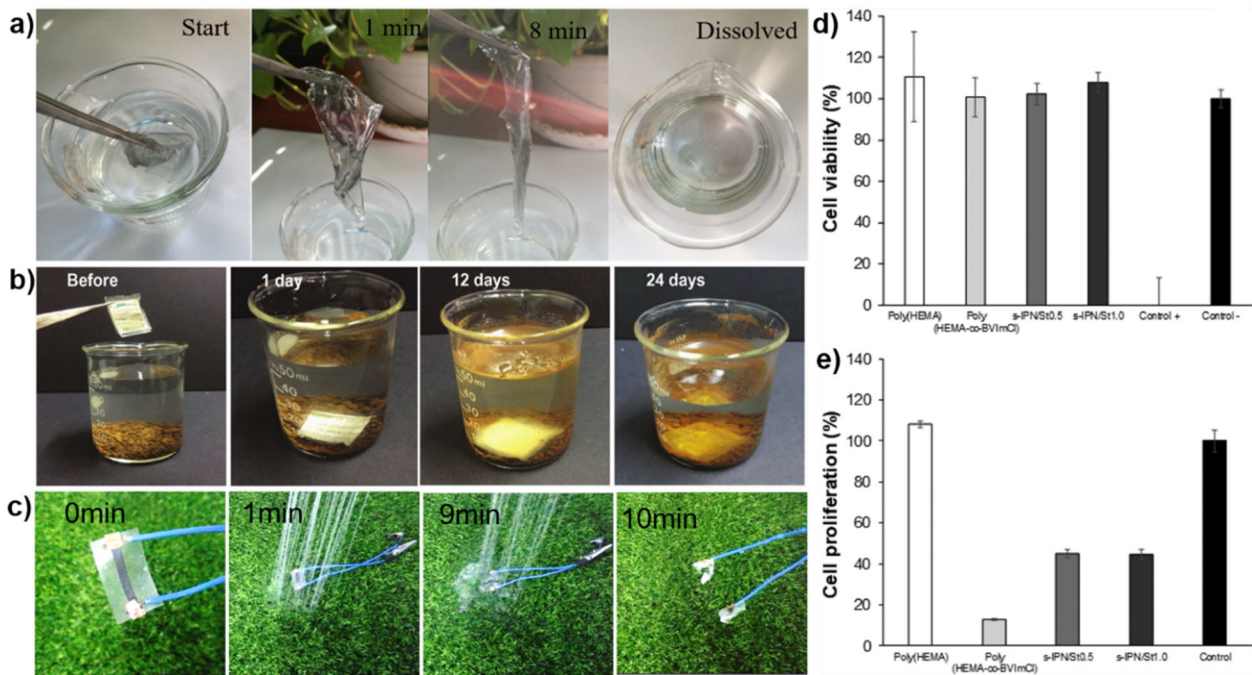


**Fig. 10 Degradability and biocompatibility of starch-based FEs.** **a** Dissolution behaviors of the starch-based conductive film. Reproduced with permission<sup>38</sup>. Copyright 2018, American Chemical Society. **b** Biodegradability tests of the starch-based device in fishbowl water. Reproduced with permission<sup>33</sup>. Copyright 2017, Wiley. **c** Degradation of the starch-based sensor under water flushing. Reproduced with permission<sup>37</sup>. Copyright 2020, American Chemical Society. **d, e** The cell viability and the cell proliferation data of the hydrogels tested against fibroblasts. Reproduced with permission<sup>45</sup>. Copyright 2019, American Chemical Society.

after the degradation of starch. But solid protocols need to be addressed in the future research.

Except for degradability, the biocompatibility of the starch-based FEs was also concerned especially for medical applications, which can be confirmed through cytotoxicity tests<sup>45,163</sup>. The cell viability and the cell proliferation assays of the starch-based hydrogels were checked using Balb/3T3 fibroblasts cell in Kanaan's work (Fig. 10d, e)<sup>43</sup>. The cell viabilities (~100%) for all starch-containing hydrogels after 48 h direct contacting were around 100%. The cell proliferation increased approximately 20% for the sample in the presence of starch. These results suggest that the FEs based on starch are degradable in natural environments and biocompatible in human body, thus may be free of e-waste and find applications in biomedical therapies.

## CONCLUSIONS AND OUTLOOKS

In summary, comparing with traditional flexible materials such as PET or PI films, starch has significant advantages including low cost, controllable biodegradability, easy processability and acceptable biocompatibility, which make it versatile in future green electronics. Starch can work as flexible substrates, electrodes, carbon source, dispersants, stabilizers, or modifier of conductive materials. In the most of its applications, starch appears in the form of thin films or gels. The electronic products may be included but not limited as flexible electrodes, sensors, supercapacitors and nanogenerators. However, there are still some problems need to be resolved despite abundant recent breakthroughs have been made.

Firstly, the mechanical property of the starch films/gels need to be strengthened in some occasions when the mechanical robustness is required. Some physic and chemical strategies were developed to date. For an example, small molecules such as ethylene glycol was usually used as plasticizers of the starch film to improve the toughness<sup>37</sup>. PVA with cross-linkers was added into the starch film to increase the tensile strength and solvent

resistance of starch substrate for FEs<sup>33</sup>. In addition, the molecular chains of the starch can be grafted with polymers, which may also achieve high mechanical strength. But the chemical modification may also bring other problem, such as the degradability. The synthesized degradable polymers such as polylactic acid (PLA) or poly (butyleneadipate-co-terephthalate) (PBAT) may be good choices to reinforce the starch-based materials<sup>164–166</sup>.

Secondly, the additional components in starch-based electronics may increase the concerns for their biocompatibility and hinder their biomedical applications. For instance, the metals, nanowires, or conductive polymers that were used to improve the electrical conductivity. The investigations on the toxicology of such materials in FEs need to be promoted urgently, in which the biologist should be involved. Some metals and metal alloys have been found to be bioabsorbable and widely used in temporary biomedical implants<sup>167</sup>. On the other hand, if the conductive materials were chemical modified or enveloped with biocompatible molecules, the toxicity may be significantly lowered down to the acceptable level, thus meeting the requirements of diagnose or therapy.

Thirdly, the starch is degradable in the nature environment, but the complete degradation of FEs may not be practical. One way to reach the totally degradation may be the using of organic conductive polymers. Otherwise, the non-degradable materials including metals, graphene, carbon nanotubes need to be recycled in the future when the starch-base FEs are widely used. Zhou and coworkers<sup>168</sup> recycled liquid metal form FEs after dissolving the soft substrate, which supplied a clue for the recycle of the non-degradable component in the FEs.

Fourthly, starch-based electronics can be gradually degraded in water or biological fluid, also implying that they might be impacted by external environment during working. In general, the life-time of the FEs may be not too long. How to make their reliable life-time be controlled remains an open question. Spiridon et al.<sup>169</sup> studied the degradation behavior of PVA/starch composite film, finding that the enzyme and nanoparticles

influenced the degradation rate. Further investigation is highly desired in the future to explore more methods to manipulate the degradation of starch-based FEs.

Last but not the least, the self-powered systems or devices that do not require external power sources, may provide the possibility for reliable outdoor electronics. Starch-based self-powered electronics can provide independent, continuous power to the FEs. For instance, Sarkar et al.<sup>24,26</sup> prepared triboelectric nanogenerator based on thermoplastic starch<sup>39,40</sup>. Such products are increasingly favored by more and more applications, but their development is still in the infancy stage. More portable and sensitive self-powered devices need to be further explored.

The work is far from done, however, it is convincing that more and more practical FE products based on starch will be developed in the future with further efforts putting into this exciting area, since the great potentials have been widely recognized. It is also of the great significance to the global green and sustainable development that is concerned by human beings.

Received: 21 July 2021; Accepted: 19 January 2022;

Published online: 03 March 2022

## REFERENCES

- Xu, Y. et al. Recent advances in flexible organic synaptic transistors. *Adv. Electron. Mater.* **7**, 2100336 (2021).
- Wang, C., Wang, C., Huang, Z. & Xu, S. Materials and structures toward soft electronics. *Adv. Mater.* **30**, 1801368 (2018).
- Huang, S., Liu, Y., Zhao, Y., Ren, Z. & Guo, C. F. Flexible electronics: stretchable electrodes and their future. *Adv. Funct. Mater.* **29**, 1805924 (2018).
- Wang, L., Wang, K., Lou, Z., Jiang, K. & Shen, G. Plant-based modular building blocks for “green” electronic skins. *Adv. Funct. Mater.* **28**, 1804510 (2018).
- Niu, Y. et al. The new generation of soft and wearable electronics for health monitoring in varying environment: from normal to extreme conditions. *Mater. Today* **41**, 219–242 (2020).
- Pierre Claver, U. & Zhao, G. Recent progress in flexible pressure sensors based electronic skin. *Adv. Eng. Mater.* **23**, 2001187 (2021).
- Li, Z., Chang, S., Khuje, S. & Ren, S. Recent advancement of emerging nano copper-based printable flexible hybrid electronics. *ACS Nano* **15**, 6211–6232 (2021).
- Zhang, H. et al. Flexible and stretchable microwave electronics: past, present, and future perspective. *Adv. Mater. Technol.* **6**, 2000759 (2020).
- Zhong, J. et al. Flexible PET/EVA-based piezoelectret generator for energy harvesting in harsh environments. *Nano Energy* **37**, 268–274 (2017).
- Hu, X. et al. Highly sensitive P(VDF-TrFE)/BTO nanofiber-based pressure sensor with dense stress concentration microstructures. *ACS Appl. Polym. Mater.* **2**, 4399–4404 (2020).
- Xu, T. et al. Three-dimensional and ultralight sponges with tunable conductivity assembled from electrospun nanofibers for a highly sensitive tactile pressure sensor. *J. Mater. Chem. C* **5**, 10288–10294 (2017).
- Ge, G. et al. Muscle-inspired self-healing hydrogels for strain and temperature sensor. *ACS Nano* **14**, 218–228 (2020).
- Liu, M. et al. Large-area all-textile pressure sensors for monitoring human motion and physiological signals. *Adv. Mater.* **29**, 1703700 (2017).
- Zhang, R., Ding, J., Liu, C. & Yang, E.-H. Highly stretchable supercapacitors enabled by interwoven CNTs partially embedded in PDMS. *ACS Appl. Energy Mater.* **1**, 2048–2055 (2018).
- Parmegiani, M. et al. PDMS/Polyimide composite as an elastomeric substrate for multifunctional laser-induced graphene electrodes. *ACS Appl. Mater. Interfaces* **11**, 33221–33230 (2019).
- Vanessa F., Balde C. P., Ruediger K. & Garam B. The Global E-waste Monitor 2020. *United Nations University (UNU)/United Nations Institute for Training and Research (UNITAR)—co-hosted SCYCLE Programme, International Telecommunication Union (ITU) & International Solid Waste Association (ISWA), Bonn/Geneva/Rotterdam* (2020).
- Li, W. et al. Biodegradable materials and green processing for green electronics. *Adv. Mater.* **32**, 2001591 (2020).
- Jian, M., Zhang, Y. & Liu, Z. Natural biopolymers for flexible sensing and energy devices. *Chin. J. Polym. Sci.* **38**, 459–490 (2020).
- Liu, H. et al. A flexible multimodal sensor that detects strain, humidity, temperature, and pressure with carbon black and reduced graphene oxide hierarchical composite on paper. *ACS Appl. Mater. Interfaces* **11**, 40613–40619 (2019).
- Feng, J.-X. et al. Flexible cellulose paper-based asymmetrical thin film supercapacitors with high-performance for electrochemical energy storage. *Adv. Funct. Mater.* **24**, 7093–7101 (2014).
- Zhao, D. et al. Cellulose-based flexible functional materials for emerging intelligent electronics. *Adv. Mater.* **33**, 2000619 (2020).
- Wang, Y., Zhang, L., Zhou, J. & Lu, A. Flexible and transparent cellulose-based ionic film as a humidity sensor. *ACS Appl. Mater. Interfaces* **12**, 7631–7638 (2020).
- Yu, H. et al. Binding conductive ink initiatively and strongly: transparent and thermally stable cellulose nanopaper as a promising substrate for flexible electronics. *ACS Appl. Mater. Interfaces* **11**, 20281–20290 (2019).
- Zhang, H., Sun, X., Hubbe, M. & Pal, L. Flexible and pressure-responsive sensors from cellulose fibers coated with multiwalled carbon nanotubes. *ACS Appl. Electron. Mater.* **1**, 1179–1188 (2019).
- Xu, X. et al. Flexible, highly graphitized carbon aerogels based on bacterial cellulose/lignin: catalyst-free synthesis and its application in energy storage devices. *Adv. Funct. Mater.* **25**, 3193–3202 (2015).
- Park, Y. & Lee, J. S. Flexible multistate data storage devices fabricated using natural lignin at room temperature. *ACS Appl. Mater. Interfaces* **9**, 6207–6212 (2017).
- Lee, D.-W., Jin, M.-H., Park, J.-H., Lee, Y.-J. & Choi, Y.-C. Flexible synthetic strategies for lignin-derived hierarchically porous carbon materials. *ACS Sustain. Chem. Eng.* **6**, 10454–10462 (2018).
- Peng, Z., Zou, Y., Xu, S., Zhong, W. & Yang, W. High-performance biomass-based flexible solid-state supercapacitor constructed of pressure-sensitive lignin-based and cellulose hydrogels. *ACS Appl. Mater. Interfaces* **10**, 22190–22200 (2018).
- Jha, S. et al. Design and synthesis of lignin-based flexible supercapacitors. *ACS Sustain. Chem. Eng.* **8**, 498–511 (2019).
- Mandal, S. et al. Protein-based flexible moisture-induced energy-harvesting devices as self-biased electronic. *Sens. ACS Appl. Electron. Mater.* **2**, 780–789 (2020).
- Talebi, S. et al. Printed-circuit-board-based two-electrode system for electronic characterization of proteins. *ACS omega* **5**, 7802–7808 (2020).
- Moudgil, A., Kalyani, N., Sinsinbar, G., Das, S. & Mishra, P. S-Layer protein for resistive switching and flexible nonvolatile memory device. *ACS Appl. Mater. Interfaces* **10**, 4866–4873 (2018).
- Jeong, H. et al. Novel eco-friendly starch paper for use in flexible, transparent, and disposable organic electronics. *Adv. Funct. Mater.* **28**, 1704433 (2018).
- Wang, C.-C., Liang, J., Liao, Y.-H. & Lu, S.-Y. 3D Porous graphene nanostructure from a simple, fast, scalable process for high performance flexible gel-type supercapacitors. *ACS Sustain. Chem. Eng.* **5**, 4457–4467 (2017).
- Raeis-Hosseini, N. & Lee, J.-S. Controlling the resistive switching behavior in starch-based flexible biomemristors. *ACS Appl. Mater. Interfaces* **8**, 7326–7332 (2016).
- Hartmann, F., Baumgartner, M. & Kaltenbrunner, M. Becoming sustainable, the new frontier in soft robotics. *Adv. Mater.* **33**, 2004413 (2021).
- Liu, H. et al. Flexible and degradable multimodal sensor fabricated by transferring laser-induced porous carbon on starch film. *ACS Sustain. Chem. Eng.* **8**, 527–533 (2019).
- Miao, J., Liu, H., Li, Y. & Zhang, X. Biodegradable transparent substrate based on edible starch-chitosan embedded with nature-inspired three-dimensionally interconnected conductive nanocomposites for wearable green electronics. *ACS Appl. Mater. Interfaces* **10**, 23037–23047 (2018).
- Chen, T. et al. Triboelectric self-powered wearable flexible patch as 3d motion control interface for robotic manipulator. *ACS nano* **12**, 11561–11571 (2018).
- Sarkar, P. K., Kamila, T. & Acharya, S. Introduction of triboelectric positive bioplastic for powering portable electronics and self-powered gait sensor. *ACS Appl. Energy Mater.* **2**, 5507–5514 (2019).
- Chen, Y., Dai, G. & Gao, Q. Starch nanoparticles–graphene aerogels with high supercapacitor performance and efficient Adsorption. *ACS Sustain. Chem. Eng.* **7**, 14064–14073 (2019).
- Le Corre, D., Bras, J. & Dufresne, A. Starch nanoparticles: a review. *Biomacromolecules* **11**, 1139–1153 (2010).
- Mekonnen, T., Mussoni, P., Khalil, H. & Bressler, D. Progress in bio-based plastics and plasticizing modifications. *J. Mater. Chem. A* **1**, 13379 (2013).
- Mohammadi Nafchi, A., Moradpour, M., Saeidi, M. & Alias, A. K. Thermoplastic starches: properties, challenges, and prospects. *Starke* **65**, 61–72 (2013).
- Kanaan, A. F. et al. Sustainable electro-responsive semi-interpenetrating starch/ionic liquid copolymer networks for the controlled sorption/release of biomolecules. *ACS Sustain. Chem. Eng.* **7**, 10516–10532 (2019).
- Patil, N. V. & Netravali, A. N. Nonedible starch based “green” thermoset resin obtained via esterification using a green catalyst. *ACS Sustain. Chem. Eng.* **4**, 1756–1764 (2016).

47. Gilet, A. et al. Synthesis of 2-hydroxydodecyl starch ethers: importance of the purification process. *Ind. Eng. Chem. Res.* **58**, 2437–2444 (2018).
48. Zheng, P., Ma, T. & Ma, X. Fabrication and properties of starch-grafted graphene nanosheet/plasticized-starch composites. *Ind. Eng. Chem. Res.* **52**, 14201–14207 (2013).
49. Xu, H., Canisag, H., Mu, B. & Yang, Y. Robust and flexible films from 100% starch cross-linked by biobased disaccharide derivative. *ACS Sustain. Chem. Eng.* **3**, 2631–2639 (2015).
50. Wu, Q., Chen, X., Zhang, Y., Wu, Z. & Huang, Y. Tough thermoplastic starch modified with polyurethane microparticles: the effects of processing temperatures. *Ind. Eng. Chem. Res.* **50**, 2008–2014 (2011).
51. Zhang, Y., Huang, Y., Chen, X., Wu, Z. & Wu, Q. Tough thermoplastic starch modified with polyurethane microparticles: the effects of NCO content in prepolymers. *Ind. Eng. Chem. Res.* **50**, 11906–11911 (2011).
52. Liircks, J. Properties and applications of compostable starch-based plastic material. *Polym. Degrad. Stab.* **59**, 245–249 (1998).
53. Ogunsona, E., Ojogbo, E. & Mekonnen, T. Advanced material applications of starch and its derivatives. *Eur. Polym. J.* **108**, 570–581 (2018).
54. Selvaraj, T. et al. The recent development of polysaccharides biomaterials and their performance for supercapacitor applications. *Mater. Res. Bull.* **126**, 110839 (2020).
55. García, N. L., Ribba, L., Dufresne, A., Aranguren, M. & Goyanes, S. Effect of glycerol on the morphology of nanocomposites made from thermoplastic starch and starch nanocrystals. *Carbohydr. Polym.* **84**, 203–210 (2011).
56. Aqlil, M. et al. Graphene oxide filled lignin/starch polymer bionanocomposite: structural, physical, and mechanical studies. *J. Agric. Food Chem.* **65**, 10571–10581 (2017).
57. de Azevedo, L. C. et al. Biodegradable films derived from corn and potato starch and study of the effect of silicate extracted from sugarcane waste ash. *ACS Appl. Polym. Mater.* **2**, 2160–2169 (2020).
58. Kaur, H. et al. Novel biodegradable films with extraordinary tensile strength and flexibility provided by nanoparticles. *ACS Sustain. Chem. Eng.* **1**, 127–136 (2012).
59. Zhang, B. et al. Facile preparation of starch-based electroconductive films with ionic liquid. *ACS Sustain. Chem. Eng.* **5**, 5457–5467 (2017).
60. Wang, T. et al. Novel biodegradable and ultra-flexible transparent conductive film for green light OLED devices. *Carbon* **172**, 379–389 (2021).
61. Prusty, G., Das, R. & Swain, S. K. Influence of functionalized single-walled carbon nanotubes on morphology, conducting and oxygen barrier properties of poly (acrylonitrile-co-starch). *Compos. B: Eng.* **62**, 236–241 (2014).
62. Qin, Y. et al. Self-assembly of metal–phenolic networks as functional coatings for preparation of antioxidant, antimicrobial, and pH-sensitive-modified starch nanoparticles. *ACS Sustain. Chem. Eng.* **7**, 17379–17389 (2019).
63. Haaj, S. B., Thielemans, W., Magnin, A. & Boufi, S. Starch nanocrystal stabilized pickering emulsion polymerization for nanocomposites with improved performance. *ACS Appl. Mater. Interfaces* **6**, 8263–8273 (2014).
64. Pereda, M., El Kissi, N. & Dufresne, A. Extrusion of polysaccharide nanocrystal reinforced polymer nanocomposites through compatibilization with poly(ethylene oxide). *ACS Appl. Mater. Interfaces* **6**, 9365–9375 (2014).
65. Zhu, G., Dufresne, A. & Lin, N. Humidity-sensitive and conductive nanopapers from plant-derived proteins with a synergistic effect of platelet-like starch nanocrystals and sheet-like graphene. *ACS Sustain. Chem. Eng.* **5**, 9431–9440 (2017).
66. Gürler, N. & Torğut, G. Graphene-reinforced potato starch composite films: improvement of mechanical, barrier and electrical properties. *Polym. Compos.* **42**, 173–180 (2020).
67. Nordin, N., Othman, S. H., Rashid, S. A. & Basha, R. K. Effects of glycerol and thymol on physical, mechanical, and thermal properties of corn starch films. *Food Hydrocoll.* **106**, 105884 (2020).
68. Moltó, J. et al. Pollutant emissions during the pyrolysis and combustion of starch/poly(vinyl alcohol) biodegradable films. *Chemosphere* **256**, 127107 (2020).
69. Lu, H. et al. Preparation of borax cross-linked starch nanoparticles for improvement of mechanical properties of maize starch films. *J. Agric. Food Chem.* **67**, 2916–2925 (2019).
70. Cataldi, P. et al. Foldable conductive cellulose fiber networks modified by graphene nanoplatelet-bio-based composites. *Adv. Electron. Mater.* **1**, 1500224 (2015).
71. Bacalzo, N. P. et al. Controlled microwave-hydrolyzed starch as a stabilizer for green formulation of aqueous gold nanoparticle ink for flexible printed electronics. *ACS Appl. Nano Mater.* **1**, 1247–1256 (2018).
72. Ren, H. et al. Transfer-medium-free nanofiber-reinforced graphene film and applications in wearable transparent pressure sensors. *ACS Nano* **13**, 5541–5548 (2019).
73. Wang, S. et al. Magnetic-assisted transparent and flexible percolative composite for highly sensitive piezoresistive sensor via hot embossing technology. *ACS Appl. Mater. Interfaces* **11**, 48331–48340 (2019).
74. Liu, W. et al. Piezoresistive pressure sensor based on synergistical innerconnect polyvinyl alcohol nanowires/wrinkled graphene film. *Small* **14**, 1704149 (2018).
75. Tiefenauer, R. F. et al. Monolayer graphene coupled to a flexible plasmonic nanograting for ultrasensitive strain monitoring. *Small* **14**, 1801187 (2018).
76. Han, Z. et al. Ultralow-cost, highly sensitive, and flexible pressure sensors based on carbon black and airlaid paper for wearable electronics. *ACS Appl. Mater. Interfaces* **11**, 33370–33379 (2019).
77. Singh, E., Meyyappan, M. & Nalwa, H. S. Flexible graphene-based wearable gas and chemical sensors. *ACS Appl. Mater. Interfaces* **9**, 34544–34586 (2017).
78. Cho, K. H., Jang, J. & Lee, J. S. Comparative study on the formation and oxidation-level control of three-dimensional conductive nanofilms for gas sensor applications. *ACS Omega* **5**, 2992–2999 (2020).
79. Wu, J. et al. Three-dimensional graphene hydrogel decorated with SnO<sub>2</sub> for high-performance NO<sub>2</sub> sensing with enhanced immunity to humidity. *ACS Appl. Mater. Interfaces* **12**, 2634–2643 (2020).
80. Xu, M. & Yadavalli, V. K. Flexible biosensors for the impedimetric detection of protein targets using silk-conductive polymer biocomposites. *ACS Sens.* **4**, 1040–1047 (2019).
81. He, X., Zhou, X., Liu, W., Liu, Y. & Wang, X. Flexible DNA hydrogel SERS active biofilms for conformal ultrasensitive detection of uranyl ions from aquatic products. *Langmuir* **36**, 2930–2936 (2020).
82. Kim, H. U. et al. Flexible MoS<sub>2</sub>-polyimide electrode for electrochemical biosensors and their applications for the highly sensitive quantification of endocrine hormones: PTH, T3, and T4. *Anal. Chem.* **92**, 6327–6333 (2020).
83. Liao, X. et al. Flexible and highly sensitive strain sensors fabricated by pencil drawn for wearable monitor. *Adv. Funct. Mater.* **25**, 2395–2401 (2015).
84. Sun, Q. et al. Active matrix electronic skin strain sensor based on piezopotential-powered graphene transistors. *Adv. Mater.* **27**, 3411–3417 (2015).
85. Atalay, O. et al. A highly stretchable capacitive-based strain sensor based on metal deposition and laser rastering. *Adv. Mater. Technol.* **2**, 1700081 (2017).
86. Liu, S. et al. Recyclable and flexible starch-Ag networks and its application in joint sensor. *Nanoscale Res. Lett.* **14**, 127 (2019).
87. Jodar, L. V., Santos, F. A., Zucolotto, V. & Janegitz, B. C. Electrochemical sensor for estriol hormone detection in biological and environmental samples. *J. Solid State Electrochem.* **22**, 1431–1438 (2017).
88. Mauruto de Oliveira, G. C. et al. Tapioca biofilm containing nitrogen-doped titanium dioxide nanoparticles for electrochemical detection of 17-β estradiol. *Electroanalysis* **29**, 2638–2645 (2017).
89. Delgado, K. P., Raymundo-Pereira, P. A., Campos, A. M., Oliveira, O. N. & Janegitz, B. C. Ultralow cost electrochemical sensor made of potato starch and carbon black nanoballs to detect tetracycline in waters and milk. *Electroanalysis* **30**, 2153–2159 (2018).
90. Orzari, L. O., Santos, F. A. & Janegitz, B. C. Manioc starch thin film as support of reduced graphene oxide: A novel architecture for electrochemical sensors. *J. Electroanal. Chem.* **823**, 350–358 (2018).
91. Camargo, J. R. et al. Electrochemical biosensor made with tyrosinase immobilized in a matrix of nanodiamonds and potato starch for detecting phenolic compounds. *Anal. Chim. Acta* **1034**, 137–143 (2018).
92. Zambianco, N. A., Silva, T. A., Zanin, H., Fatibello-Filho, O. & Janegitz, B. C. Novel electrochemical sensor based on nanodiamonds and manioc starch for detection of diquat in environmental samples. *Diam. Relat. Mater.* **98**, 107512 (2019).
93. Stanford, M. G., Yang, K., Chyan, Y., Kittrell, C. & Tour, J. M. Laser-induced graphene for flexible and embeddable gas sensors. *ACS Nano* **13**, 3474–3482 (2019).
94. Zito, C. A., Perfecto, T. M., Dippel, A.-C., Volanti, D. P. & Koziej, D. Low-temperature carbon dioxide gas sensor based on yolk-shell ceria nanospheres. *ACS Appl. Mater. Interfaces* **12**, 17745–17751 (2020).
95. Kumar, R., Zheng, W., Liu, X., Zhang, J. & Kumar, M. MoS<sub>2</sub>-based nanomaterials for room-temperature gas sensors. *Adv. Mater. Technol.* **5**, 1901062 (2020).
96. Chathuranga, H. et al. Multifunctional, bioinspired, and moisture responsive graphene oxide/tapioca starch nanocomposites. *Adv. Mater. Technol.* **7**, 2100447 (2021).
97. Kumar, B., Castro, M. & Feller, J.-F. Tailoring the chemo-resistive response of self-assembled polysaccharide-CNT sensors by chain conformation at tunnel junctions. *Carbon* **50**, 3627–3634 (2012).
98. Peregrino, P. P. et al. Starch-mediated immobilization, photochemical reduction, and gas sensitivity of graphene oxide films. *ACS Omega* **5**, 5001–5012 (2020).
99. Hua, Q. et al. Skin-inspired highly stretchable and conformable matrix networks for multifunctional sensing. *Nat. Commun.* **9**, 244 (2018).
100. Wang, Q. et al. Self-healable multifunctional electronic tattoos based on silk and graphene. *Adv. Funct. Mater.* **29**, 1808695 (2019).
101. Kumar, S., Manikandan, V. S., Palai, A. K., Mohanty, S. & Nayak, S. K. Fe<sub>2</sub>O<sub>3</sub> as an efficient filler in PVDF-HFP based polymeric electrolyte for dye sensitized solar cell application. *Solid State Ion.* **332**, 10–15 (2019).

102. Lin, Z., Xiang, X., Peng, S., Jiang, X. & Hou, L. Facile synthesis of chitosan-based carbon with rich porous structure for supercapacitor with enhanced electrochemical performance. *J. Electroanal. Chem.* **823**, 563–572 (2018).
103. Pal, P. & Ghosh, A. Investigation of ionic conductivity and relaxation in plasticized PMMA-LiClO<sub>4</sub> solid polymer electrolytes. *Solid State Ion.* **319**, 117–124 (2018).
104. Siyal, S. H. et al. Ultraviolet irradiated PEO/LATP composite gel polymer electrolytes for lithium-metallic batteries (LMBs). *Appl. Surf. Sci.* **494**, 1119–1126 (2019).
105. Wang, D.-d et al. Evolution process of the plasma electrolytic oxidation (PEO) coating formed on aluminum in an alkaline sodium hexametaphosphate ( $\text{NaPO}_3)_6$ ) electrolyte. *J. Alloy. Compd.* **798**, 129–143 (2019).
106. Chauhan, J. K., Kumar, M., Yadav, M., Tiwari, T. & Srivastava, N. Effect of NaClO<sub>4</sub> concentration on electrolytic behaviour of corn starch film for supercapacitor application. *Ionics* **23**, 2943–2949 (2017).
107. Chen, T. & Liu, Z. Starch-assistant synthesis of Ni quantum dots/ultrathin carbon nanosheet hybrids for high performance supercapacitor. *Mater. Lett.* **236**, 248–251 (2019).
108. Chen, S., Jiang, J., Xu, F. & Gong, S. Crepe cellulose paper and nitrocellulose membrane-based triboelectric nanogenerators for energy harvesting and self-powered human-machine interaction. *Nano Energy* **61**, 69–77 (2019).
109. Wen, Z. et al. A wrinkled PEDOT:PSS film based stretchable and transparent triboelectric nanogenerator for wearable energy harvesters and active motion sensors. *Adv. Funct. Mater.* **28**, 1803684 (2018).
110. Zhang, R. et al. Human body constituted triboelectric nanogenerators as energy harvesters, code transmitters, and motion sensors. *ACS Appl. Energy Mater.* **1**, 2955–2960 (2018).
111. Chen, B., Yang, Y. & Wang, Z. L. Scavenging wind energy by triboelectric nanogenerators. *Adv. Energy Mater.* **8**, 1702649 (2018).
112. Zheng, H. et al. Concurrent harvesting of ambient energy by hybrid nanogenerators for wearable self-powered systems and active remote sensing. *ACS Appl. Mater. Interfaces* **10**, 14708–14715 (2018).
113. Liang, Q. et al. Recyclable and green triboelectric nanogenerator. *Adv. Mater.* **29**, 1604961 (2017).
114. Shi, X. et al. Portable self-charging power system via integration of a flexible paper-based triboelectric nanogenerator and supercapacitor. *ACS Sustain. Chem. Eng.* **7**, 18657–18666 (2019).
115. Stanford, M. G. et al. Laser-induced graphene triboelectric nanogenerators. *ACS nano* **13**, 7166–7174 (2019).
116. Rovisco, A. et al. Piezoelectricity enhancement of nanogenerators based on PDMS and ZnSnO<sub>3</sub> nanowires through microstructuration. *ACS Appl. Mater. Interfaces* **12**, 18421–18430 (2020).
117. Fan, F.-R., Tian, Z.-Q. & Lin Wang, Z. Flexible triboelectric generator. *Nano Energy* **1**, 328–334 (2012).
118. Khandelwal, G., Joseph Raj, N. P. M., Alluri, N. R. & Kim, S.-J. Enhancing hydrophobicity of starch for biodegradable material-based triboelectric nanogenerators. *ACS Sustain. Chem. Eng.* **9**, 9011–9017 (2021).
119. Bao, Y., Wang, R., Lu, Y. & Wu, W. Lignin biopolymer based triboelectric nanogenerators. *APL Mater.* **5**, 074109 (2017).
120. Zhu, Z., Xia, K., Xu, Z., Lou, H. & Zhang, H. Starch paper-based triboelectric nanogenerator for human perspiration sensing. *Nanoscale Res. Lett.* **13**, 365 (2018).
121. Ccorahua, R., Cordero, A., Luyo, C., Quintana, M. & Vela, E. Starch-cellulose-based triboelectric nanogenerator obtained by a low-cost cleanroom-free processing method. *MRS Adv.* **4**, 1315–1320 (2019).
122. Ccorahua, R., Huaroto, J., Luyo, C., Quintana, M. & Vela, E. A. Enhanced-performance bio-triboelectric nanogenerator based on starch polymer electrolyte obtained by a cleanroom-free processing method. *Nano Energy* **59**, 610–618 (2019).
123. Kim, S. J. & Lee, J. S. Flexible organic transistor memory devices. *Nano Lett.* **10**, 2884–2890 (2010).
124. Zhao, J. et al. Flexible organic tribotronic transistor for pressure and magnetic sensing. *ACS Nano* **11**, 11566–11573 (2017).
125. Yeo, S. Y., Park, S., Yi, Y. J., Kim, D. H. & Lim, J. A. Highly sensitive flexible pressure sensors based on printed organic transistors with centro-apically self-organized organic semiconductor microstructures. *ACS Appl. Mater. Interfaces* **9**, 42996–43003 (2017).
126. Torikai, K., Furlan de Oliveira, R., Starnini de Camargo, D. H. & Bof Bufon, C. C. Low-voltage, flexible, and self-encapsulated ultracompact organic thin-film transistors based on nanomembranes. *Nano Lett.* **18**, 5552–5561 (2018).
127. Mariani, F., Gualandi, I., Tessarolo, M., Fraboni, B. & Scavetta, E. PEDOT: Dye-based, flexible organic electrochemical transistor for highly sensitive pH monitoring. *ACS Appl. Mater. Interfaces* **10**, 22474–22484 (2018).
128. Shao, F., Cai, M.-L., Gu, X.-F. & Wu, G.-D. Starch as ion-based gate dielectric for oxide thin film transistors. *Org. Electron.* **45**, 203–208 (2017).
129. Valov, I. et al. Nanobatteries in redox-based resistive switches require extension of memristor theory. *Nat. Commun.* **4**, 1771 (2013).
130. Hosseini, N. R. & Lee, J.-S. Biocompatible and flexible chitosan-based resistive switching memory with magnesium electrodes. *Adv. Funct. Mater.* **25**, 5586–5592 (2015).
131. Park, Y. & Lee, J. S. Artificial synapses with short- and long-term memory for spiking neural networks based on renewable materials. *ACS Nano* **11**, 8962–8969 (2017).
132. Qian, C., Sun, J., Yang, J. & Gao, Y. Flexible organic field-effect transistors on biodegradable cellulose paper with efficient reusable ion gel dielectrics. *RSC Adv.* **5**, 14567–14574 (2015).
133. Fan, Y., Bose, R. K. & Picchioni, F. Highly branched waxy potato starch-based polyelectrolyte: controlled synthesis and the influence of chain composition on solution rheology. *Ind. Eng. Chem. Res.* **59**, 10847–10856 (2020).
134. Gao, W. T. et al. Dendrite integration mimicked on starch-based electrolyte-gated oxide dendrite transistors. *ACS Appl. Mater. Interfaces* **10**, 40008–40013 (2018).
135. Alday, P. P. et al. Biopolymer electrolyte membranes (BioPEMs) for sustainable primary redox batteries. *Adv. Sustain. Syst.* **4**, 1900110 (2019).
136. Liu, H. et al. Biofriendly, stretchable, and reusable hydrogel electronics as wearable force sensors. *Small* **14**, 1801711 (2018).
137. Han, S. et al. Dual conductive network hydrogel for a highly conductive, self-healing, anti-freezing, and non-drying strain sensor. *ACS Appl. Polym. Mater.* **2**, 996–1005 (2020).
138. Wu, Z., Yang, X. & Wu, J. Conductive hydrogel- and organohydrogel-based stretchable sensors. *ACS Appl. Mater. Interfaces* **13**, 2128–2144 (2021).
139. Niu, Y. et al. Environmentally compatible wearable electronics based on ionically conductive organohydrogels for health monitoring with thermal compatibility, anti-dehydration, and underwater adhesion. *Small* **17**, 2101151 (2021).
140. Jiamjaryatam, R., Kongpensook, V. & Pradipasena, P. Effects of amylose content, cooling rate and aging time on properties and characteristics of rice starch gels and puffed products. *J. Cereal. Sci.* **61**, 16–25 (2015).
141. Abhari, N., Madadlou, A., Dini, A. & Hosseini Naveh, O. Textural and cargo release attributes of trisodium citrate cross-linked starch hydrogel. *Food Chem.* **214**, 16–24 (2017).
142. Villanueva, M. E. et al. Antimicrobial activity of starch hydrogel incorporated with copper nanoparticles. *ACS Appl. Mater. Interfaces* **8**, 16280–16288 (2016).
143. Ye, L. et al. Physical cross-linking starch-based zwitterionic hydrogel exhibiting excellent biocompatibility, protein resistance, and biodegradability. *ACS Appl. Mater. Interfaces* **8**, 15710–15723 (2016).
144. Ji, N. et al. Fabrication and characterization of starch nanohydrogels via reverse emulsification and internal gelation. *J. Agric Food Chem.* **66**, 9326–9334 (2018).
145. Qin, Y., Wang, J., Qiu, C., Xu, X. & Jin, Z. A dual cross-linked strategy to construct moldable hydrogels with high stretchability, good self-recovery, and self-healing capability. *J. Agric Food Chem.* **67**, 3966–3980 (2019).
146. Mao, Y. et al. Starch-based adhesive hydrogel with gel-point viscoelastic behavior and its application in wound sealing and hemostasis. *J. Mater. Sci. Technol.* **63**, 228–235 (2021).
147. Gonzalez, K. et al. Starch/graphene hydrogels via click chemistry with relevant electrical and antibacterial properties. *Carbohydr. Polym.* **202**, 372–381 (2018).
148. Wang, Y. et al. Smart window based on temperature-responsive starch hydrogel with a dynamic regulation mode. *Ind. Eng. Chem. Res.* **59**, 21012–21017 (2020).
149. Lu, J. et al. Highly tough, freezing-tolerant, healable and thermoplastic starch/poly(vinyl alcohol) organohydrogels for flexible electronic devices. *J. Mater. Chem. A* **34**, 18406–18420 (2021).
150. Zeng, S., Zhang, J., Zu, G. & Huang, J. Transparent, flexible, and multifunctional starch-based double-network hydrogels as high-performance wearable electronics. *Carbohydr. Polym.* **267**, 118198 (2021).
151. Liu, H. et al. A flexible conductive hybrid elastomer for high-precision stress/strain and humidity detection. *J. Mater. Sci. Technol.* **35**, 176–180 (2019).
152. Wang, Y. et al. Ultrafast self-healing, reusable, and conductive polysaccharide-based hydrogels for sensitive ionic sensors. *ACS Sustain. Chem. Eng.* **8**, 18506–18518 (2020).
153. Liu, P. et al. Facile preparation of eco-friendly, flexible starch-based materials with ionic conductivity and strain-responsiveness. *ACS Sustain. Chem. Eng.* **8**, 19117–19128 (2020).
154. Kong, L., Gao, Z., Li, X. & Gao, G. An amylopectin-enabled skin-mounted hydrogel wearable sensor. *J. Mater. Chem. B* **9**, 1082–1088 (2021).
155. Li, Q. et al. In situ construction of potato starch based carbon nanofiber/activated carbon hybrid structure for high-performance electrical double layer capacitor. *J. Power Sources* **207**, 199–204 (2012).
156. Zhang, K. et al. Electrochemical activity of Samarium on starch-derived porous carbon: rechargeable Li- and Al-ion batteries. *Nano Converg.* **7**, 11 (2020).
157. Pang, L. et al. One-step synthesis of high-performance porous carbon from corn starch for supercapacitor. *Mater. Lett.* **184**, 88–91 (2016).

158. Liu, M.-C. et al. Three-dimensional interconnected reticular porous carbon from corn starch by a sample sol–gel method toward high-performance supercapacitors with aqueous and ionic liquid electrolytes. *ACS Sustain. Chem. Eng.* **7**, 18690–18699 (2019).
159. Willfahrt, A., Steiner, E., Hötzl, J. & Crispin, X. Printable acid-modified corn starch as non-toxic, disposable hydrogel-polymer electrolyte in supercapacitors. *Appl. Phys. A* **125**, 474 (2019).
160. Koduru, H. K. et al. Fabrication and characterization of magnesium—ion-conducting flexible polymer electrolyte membranes based on a nanocomposite of poly(ethylene oxide) and potato starch nanocrystals. *J. Solid State Electrochem.* **25**, 2409–2428 (2021).
161. Albright, V. C. & Chai, Y. Knowledge gaps in polymer biodegradation research. *Environ. Sci. Technol.* **55**, 11476–11488 (2021).
162. Sung, W. & Nikolov, Z. L. Accelerated degradation studies of starch-filled poly-ethylene films. *Mater. Interfaces* **31**, 2332–2339 (1992).
163. Ceseracciu, L., Heredia-Guerrero, J. A., Dante, S., Athanassiou, A. & Bayer, I. S. Robust and biodegradable elastomers based on corn starch and poly-dimethylsiloxane (PDMS). *ACS Appl Mater. Interfaces* **7**, 3742–3753 (2015).
164. Ali, S. S., Tang, X., Alavi, S. & Faubion, J. Structure and physical properties of starch/poly vinyl alcohol/sodium montmorillonite nanocomposite films. *J. Agric Food Chem.* **59**, 12384–12395 (2011).
165. Kim, J.-H., Lee, J. C. & Kim, G.-H. Study on poly(butylene adipate-co-terephthalate)/starch composites with polymeric methylenediphenyl diisocyanate. *J. Appl. Polym. Sci.* **132**, 41884 (2015).
166. Wang, X. W. et al. Degradability comparison of poly(butylene adipate terephthalate) and its composites filled with starch and calcium carbonate in different aquatic environments. *J. Appl. Polym. Sci.* **136**, 1804510 (2019).
167. Ryu, H., Seo, M. H. & Rogers, J. A. Bioresorbable metals for biomedical applications: from mechanical components to electronic devices. *Adv. Health. Mater.* **10**, 2002236 (2021).
168. Teng, L. et al. Liquid metal-based transient circuits for flexible and recyclable electronics. *Adv. Funct. Mater.* **29**, 1808739 (2019).
169. Spiridon, L., Popescu, M. C., Bodarla, R. & Vasile, C. Enzymatic degradation of some nanocomposites of PVA with starch. *Polym. Degrad. Stab.* **93**, 1884–1890 (2008).

## ACKNOWLEDGEMENTS

The authors would like to thank the financial supports from the National Natural Science Foundation of China (No.21805178), Chinese Postdoctoral Science Foundation (2019M653734), Key Research and Development Program of Shaanxi Province (2021GY-305), Natural Science Foundation of Shaanxi Provincial Department of

Education (20JS062), Foundation for Selected Oversea Chinese Scholar in Shaanxi Province (No. 2017016), and the advanced research fund of SUST (2016GBJ-14).

## AUTHOR CONTRIBUTIONS

H. Xiang wrote original draft and collected the data. H. Liu conceptualized, supervised, and edited the draft. Z. Li, T. Chen, and H. Zhou reviewed the manuscript and provided scientific comments and suggestions. W. Huang provided overall supervision of the work.

## COMPETING INTERESTS

The authors declare no competing interests.

## ADDITIONAL INFORMATION

**Correspondence** and requests for materials should be addressed to Hanbin Liu or Wei Huang.

**Reprints and permission information** is available at <http://www.nature.com/reprints>

**Publisher's note** Springer Nature remains neutral with regard to jurisdictional claims in published maps and institutional affiliations.



**Open Access** This article is licensed under a Creative Commons Attribution 4.0 International License, which permits use, sharing, adaptation, distribution and reproduction in any medium or format, as long as you give appropriate credit to the original author(s) and the source, provide a link to the Creative Commons license, and indicate if changes were made. The images or other third party material in this article are included in the article's Creative Commons license, unless indicated otherwise in a credit line to the material. If material is not included in the article's Creative Commons license and your intended use is not permitted by statutory regulation or exceeds the permitted use, you will need to obtain permission directly from the copyright holder. To view a copy of this license, visit <http://creativecommons.org/licenses/by/4.0/>.

© The Author(s) 2022